# Data Processing Report

for


## Area: OTWAY BASIN

Permits: VIC/P37(v) and VIC/P44
Project: Antares 3D and Multivintage Reprocessing 2003

WG Contract Number: J2697
Date: August 2004


**WesternGeco**
Level 5, 256 St Georges Terrace, Perth, Western Australia 6000, Australia

**Report Author**
Monica Wurfel

# *Table of Contents*

# *TABLE OF FIGURES*

# 1.0 Introduction

This report details the 2004 data processing by WesternGeco of the Antares 3D Marine Seismic Survey covering parts of the VIC/P37 (v) and VIC/P44 in the Otway Basin between Port Campbell and Warrnambool. The Marine Vessel Orient Explorer acquired the data during October/November 2003. Acquisition parameters can be found in **Appendix 4.1**.

The objectives of the Antares 3D survey are a detailed image of complex faulted structures whilst preserving as close to true amplitude as possible. Also producing a fully migrated image up to the southern permit boundary by incorporating a 3km wide apron of the Casino 3D dataset pre-stack and creating a seamless merge with the Minerva 3D dataset pre-stack.

The project covered a total of ~414km$^2$ of data consisting of approximately 209km$^2$ of Antares, approximately 30km$^2$ of Casino (thin strip to attain full fold full migration to permit boundary) and approximately 175km$^2$ of Minerva data.

The project supervisor for WOODSIDE was Rob Eliott-Lockhart. Tan King Seong managed the project for WesternGeco with geophysical support from Richard Bisley. Parameter testing and production for the project was performed by Monica Wurfel.

The data were processed through a sequence which included swell noise attenuation, linear noise removal and tau-p deconvolution, adjacent trace sum, inverse Q, high resolution radon demultiples, phase/amplitude matching, fold regularisation, pre-stack time Kirchhoff migration, including four passes of velocity analysis.

# 2.0 Seismic Data Processing

## 2.1 Reformat SEG-D to Omega

The de-multiplexed field data were reformatted from SEG-D to an in-house source-gathered seismic file format. Full word, 32 bit floating point data at geophone amplitude was maintained.

Diagnostics from the transcription programme list input and output record numbers, plus parity and block length errors. Each printout was checked against the observer logs to ensure that all the data had been correctly transcribed. Selected shot records and a near trace section were displayed for quality control on each line.

## 2.2 Navigation/Seismic Data Merge

The navigation geometry information was used to update the seismic trace headers. The two sets of data were matched using unique shot point and detector numbers. While the navigation values were stored in the data trace headers, nominal values from 2D geometry were actually used in the data processing as they had the benefit of being regular compared to real navigation values.

## 2.3 Resample

An anti-alias filter was applied and the data resampled.

Parameter values:
Input Sampling Interval : 2 ms
Output Sampling Interval : 4 ms

| Anti-alias Filter: | |
|---|---|
| Phase | : Minimum |
| Cutoff Frequency | : 100 Hz |
| Cutoff Slope | : 72 dB/octave |

## 2.4 Minimum Phase Low-Cut Filter

A band-pass filter was described by low -cut frequencies and associated dB/octave cutoff slopes. The specified cutoff frequencies are located at the half-power (-3 dB in amplitude) response points and the slopes at these frequencies are equal to the respective dB/octave values. The slope is an approximate cosine squared function in the amplitude domain. The filter was normalized so that output amplitudes were the same as input amplitudes for frequency components within the passband.

| Parameter values: | |
|---|---|
| Phase | : Minimum |
| Low-cut Frequency | : 4 Hz |
| Low-cut Slope | : 18 dB/octave |

## 2.5 Field Data Edits

Records flagged as bad in the Observer's logs or as displayed in the near trace gather and QC plots were edited from the processing sequence.

## 2.6 Amplitude Recovery

### 2.6.1 Time Function Gain

This process scales trace samples by first raising the time (in seconds) to a user-supplied exponential value, then multiplying the result by the amplitude of the sample at that time. That is:

$$A_o(t) = A_i(t)\ t^x$$

where:

$A_o(t)$ is the amplitude of output trace sample at time $t$

$A_i(t)$ is the amplitude of input trace sample at time $t$

$t$ is the time in seconds

$x$ is the value of gain exponent

| Parameter values: |
|---|
| Exponent Value : 2 |

## 2.7 Swell Noise Attenuation (SWATT)

Swell noise is caused by rough sea conditions during data acquisition, particularly when the cables are towed at relatively shallow depths. SWATT aims to attenuate this noise by

transforming the processing gather into the frequency domain and applying a spatial median filter. Frequency bands that deviate from the median amplitude by a specified threshold are either zeroed, or replaced by good frequency bands interpolated from neighbouring traces.

Two passes of SWATT were implemented to remove as much of the noise as possible while leaving the signal component of the wavefield unharmed.

Parameter values: Pass One

| | |
|---|---|
| Processing Domain | : Shot |
| Width of Spatial Median Filter | : 21 Traces |
| Frequency Range Processed | : 0 to 40 Hz |
| Width of Frequency Bands to Process | : 5 Hz |

*Threshold Values:*

| Time (ms) | Threshold (%) |
|---|---|
| 40 | |
| 1000 | 20 |
| 3000 | 10 |
| 6144 | 5 |

Parameter values: Pass Two

| | |
|---|---|
| Processing Domain | : Shot |
| Width of Spatial Median Filter | : 11 Traces |
| Frequency Range Processed | : 0 to 10 Hz |
| Width of Frequency Bands to Process | : 5 Hz |

*Threshold Values:*

| Time (ms) | Threshold (%) |
|---|---|
| 0 | 5 |
| 1000 | 5 |
| 6144 | 5 |

## *2.8 F-K Dip Filter*

A seismic section such as a shot gather, CMP gather or stack section is a two-dimensional array of samples representing the amplitude of the seismic signal as a function of reflection time (t) and trace position (x). Dipping events (including linear noise) which overlap in this time-offset (t-x) domain cannot often be easily separated. However, a Fourier transform can be used to convert the seismic signal to the f-k domain, that is, to a function of temporal frequency (f) and spatial frequency or wavenumber (k). In this domain, dipping events plot along straight lines radiating outwards from the point of zero frequency and zero wavenumber. Gently dipping events plot closer to the frequency (vertical) axis (horizontal events actually plot along this axis); while steeply dipping events plot closer to the wavenumber (horizontal) axis. Events with a positive dip (ie, where the reflection time increases as the trace position increases) have positive wavenumbers and events with negative dips have negative wavenumbers. The events are therefore more easily separated in the f-k domain, and unwanted events such as linear noise are rejected by applying a user-specified filter. The data are then inverse Fourier transformed to the t-x domain.

The target of this filter was “mud roll”, evident in some shots from the shallower parts of the survey area. The velocities of these events were so low as to cause difficulties transforming to the linear Tau-P domain. The “mud roll” was passed by the K-F filter and subsequently subtracted from the shot gathers after transforming back to the X-T domain.

(Note: The term dip refers only to the apparent dip of an event measured in time (ms/trace) or velocity ((ft or m)/s) and not to the actual spatial dip of the geologic structure.)

Parameter values:

Velocities (specified in ms/trc) were used to define a fan-shaped pass region of f-k space.
A taper was also applied to the filter boundaries to smooth the transition between the pass and reject zones.

| | |
|---|---|
| Low Dip Cutoff | : -11.7 |
| High Dip Cutoff | : 9999 |
| Low Dip Taper (centred on the low dip cutoff) | : 7.8 |
| High Dip Taper (centred on the high dip cutoff) | : 9999 |
| Taper Type | : Cosine |
| Fan Origin | : Zero Frequency + Zero Wavenumber |

The dips were therefore attenuated by the same factor for all frequencies.

## *2.9* 3D Inline Grid

The Antares Inline 3D grid was applied to all three surveys prior to the Velocity Analysis

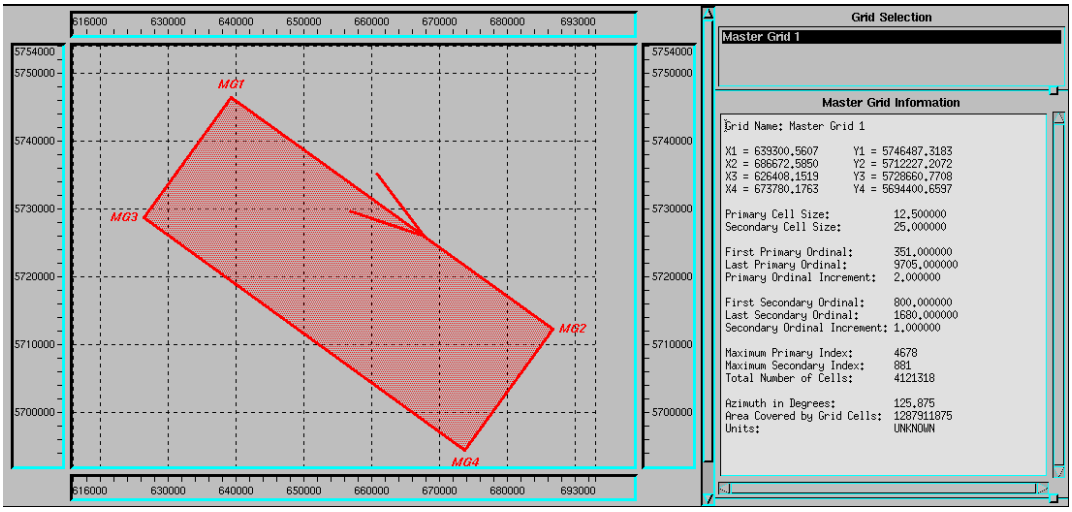


**Figure 1: 3D Inline Grid**

## *2.10 First Pass Velocity Analysis*

Velocity analysis was performed using **WesternGeco's** Interactive Velocity Processing (INVA) package. At regular intervals across the survey CMP gather data were selected. From this data Multi-Velocity Function (MVF) stacks and velocity semblance values were computed. For each velocity location, MVF data, semblances and gathers are displayed interactively allowing stacking velocities to be interpreted.

NMO-corrected gathers are then produced to check the validity of the picks and any necessary changes made before the velocity field is output.

Parameter Values:

| | |
|---|---|
| Analysis Spacing | : 4km |
| Number of CMPs per Analysis (MVF Stack) | : 15 |
| Number of CMPs per Analysis (Semblance Display) | : 3 |

## *2.11* Tau-P Linear Noise Removal & Deconvolution

### *2.11.1 Tau-P transform*

The data were forward transformed into the Tau-P (or slant-stack) domain. In this domain certain types of coherent noise can be isolated and thence inverse-transformed and subtracted. Geometry compensation is needed to reduce artefacts due to gather geometry and so improve separation of transformed events whilst maintaining acceptable invertability for the noise being modelled. Preconditioning steps may be required to reduce other artefacts that may hinder separation of noise from signal; Such artefacts can be caused by things such as data aliasing, event truncation at gather boundaries, high amplitude incoherent noise (e.g. swell noise).

Parameter Values:

Gather type : Shots

Pre-transform conditioning : Time function gain, 1:2 unaliased trace interpolation, near and far offset extrapolation and cosine taper

Geometry compensation : Least Squares, 5pc white noise
Reference offset(m) : 4058
Number p traces : 1048
Minimum p value : -2750
Maximum p value : +3250

### *2.11.2 Tau-P domain linear noise filtering*

High-energy linear and near-linear noise, which contaminated primary in the zone of interest, was suppressed by muting in the tau-p domain. The noise zone was then inverse-transformed and subtracted from the data in the t-x domain.

Parameter values:

Polygon defining noise zone:

Water bottom time 0 to 100ms:

| moveout (sec) | tau (sec) |
|---|---|
| 2.75 | 0 |
| 2.69 | 22 |
| 2.44 | 49 |
| 2.26 | 89 |
| 1.98 | 182 |
| 1.79 | 260 |
| 1.47 | 518 |
| 1.21 | 811 |
| .99 | 1135 |
| .94 | 1694 |
| .69 | 6932 |
| -.69 | 6932 |
| -.94 | 1694 |
| -.99 | 1135 |
| -1.21 | 811 |
| -1.47 | 518 |
| -1.79 | 260 |
| -1.98 | 182 |

| | |
|---|---|
| -2.26 | 89 |
| -2.44 | 49 |
| -2.69 | 22 |
| -2.75 | 0 |

### *2.11.3 Tau-P domain water bottom dependant deconvolution*

When the offset is zero and the reflectors are horizontal, a first-order multiple has a two-way time that is twice the period of the primary. However, for non-zero offset this is not the case – the multiple time is less than twice the time of the primary. Consequently, the ability of conventional Wiener-Levinson deconvolution to attenuate longer period multiples, particularly on longer offset traces, is very limited. A regular periodicity for the multiples can be imposed via a linear tau-p transform of the shot-ordered data. As the intention is to apply deconvolution in the tau-p domain, only time function gain scaling is applied to this data to ensure that the amplitude relationship between successive repeats of a multiple is preserved.

Wiener-Levinson least-squares predictive deconvolution operators were designed from autocorrelations of windows within each p-trace and were applied on a trace-by-trace basis. Start times were used to control the location of the design windows but application included all data earlier than the start time of the first window and later than the end time of the last window.

The noise model was inverse-transformed and subtracted from the data in the t-x domain.

Parameter Values:

Design window(s) : 0-2500ms

Minimum Predictive Lag : 80% predicted water bottom multiple tau period, minimum 32ms
Total Operator Length : 220% predicted water bottom multiple tau period, maximum 600ms

## 2.12 *K-Filter / Trace Reduction*

A Fourier transform was used to convert trace position to the spatial frequency (wavenumber (k)) domain. A range of wavenumbers was specified to be passed by the filter and a taper was also applied to the filter boundaries to smooth the transition between the pass and the reject regions.

After k-filtering, the number of traces in each shot record was reduced by dropping alternate traces. In this way the k-filter was used to act as an anti-aliasing filter in the wavenumber domain, attenuating energy that would otherwise have become aliased when the trace separation was doubled by the dropping of alternate traces.

For convenience, the k-filter was implemented in the f-k domain. A 2-D Fourier transform was used to convert trace position to the wavenumber domain and reflection time to the frequency (f) domain. After implementation of the k-filter the data were inverse Fourier transformed back to the t-x domain.

A second F-K filter was implemented as part of the k-filter to remove residual “mud roll” manifesting itself as linear noise.

Parameter values: Antares M3D

| | |
|---|---|
| Input Shot Records | : 324 traces |
| Output Shot Records | : 162 traces |
| High Wavenumber Cutoff | : 4.5 of k-Nyquist (relative to input trace separation) |

Taper (centred on the high wavenumber cutoff) : 0.1 of k-Nyquist

Velocities (specified in ms/trc) were used to define a fan-shaped pass region of f-k space.
A taper was also applied to the filter boundaries to smooth the transition between the pass and reject zones.

| | |
|---|---|
| Low Dip Cutoff | : -8.5 |
| High Dip Cutoff | : 5.6 |
| Low Dip Taper (centred on the low dip cutoff) | : 8.5 |
| High Dip Taper (centred on the high dip cutoff) | : 5.6 |
| Taper Type | : Cosine |

## *2.13 Inverse Q-Filter*

To compensate for the earths Q-filtering effects, (ie attenuation and dispersion of frequencies with propagation velocity) a time-variant compensation was applied using an algorithm based on the Futterman frequency-constant Q model of earth attenuation.

Amplitude compensation was applied by inverse filtering within short time windows of data. The higher frequencies within these inverse filters were gain-limited in order to prevent noise from being unduly amplified. That is, the amplitude spectrum of the filters was clipped at a maximum gain level and rolled off smoothly after that point, with a cosine-squared taper. Limiting the spectrum in this manner has the effect of restricting the amplitude treatment at a particular time to the range of frequencies over which the signal is believed to dominate the noise.

Parameter values:

| | |
|---|---|
| Compensation Type | : Phase/Amplitude |
| Q Value | : 136 |
| Maximum Gain Level | : 18dB |
| Source of Q Value | : Woodside supplied |
| Reference Frequency | : 750Hz |

## *2.14 Second Pass Velocity Analysis*

Velocity analysis was performed using **WesternGeco's** Interactive Velocity Processing (INVA) package.

NMO-corrected gathers are then produced to check the validity of the picks and any necessary changes made before the velocity field is output.

Parameter Values:

| | |
|---|---|
| Analysis Spacing | : 2 km |
| Number of CMPs per Analysis (MVF Stack) | : 15 |
| Number of CMPs per Analysis (Semblance Display) | : 3 |

## *2.15 Weighted Least Squares Radon Multiple Attenuation*

Radon Multiple Attenuation is principally a modelling and subtraction process. CMP gathers are transformed to the Radon (parabolic tau-p) domain, unwanted coherent noise is isolated in this domain, transformed back to the time-offset (t-x) domain and then subtracted from the original data. The transform separates events according to moveout (or velocity), and hence multiple

energy can be isolated in the tau-p domain (by means of a mute) provided it has a different velocity to that of the primaries.

Effective separation of coherent signal (primaries) and noise (multiples) requires that both are adequately focused in the Radon domain. Conventionally this is achieved in two steps. For a parabolic Radon transform, the first step is to condition coherent signal and noise events such that their moveout is approximately parabolic, and assumes their amplitude and phase are approximately constant across all offsets. The second step is to apply a geometry compensation filter during the transform, which attempts to reduce artefacts caused by the input gather geometry. A least-squares geometry compensation filter requires the moveout range for the transform to be adequate to model all coherent events. The transform minimises the difference between the input and the forward and reverse transformed data (the residual). If a significant amount of coherent energy lies outside the modelled moveout range, artefacts will result.

Weighted Least-Squares Radon transforms seek to improve the focusing of events in the Radon domain over that provided by the conventional transform. Prior information (derived from the data themselves) is used to create weights that improve the sparseness of the transform domain whilst still modelling all of the data. Improved focusing in the Radon domain improves identification and separation of signal and noise trends, with reduced artefact levels. For multiple attenuation, improved focusing allows the Radon domain mute to be moved closer to the primary events than with the conventional transform, and primary and multiple events with very little moveout discrimination can be separated.

Weighted Least-Squares Radon transforms can also reduce artefacts caused by data aliasing. Aliased input data lead to dispersed energy in the transform when a conventional transform is used. The weights for the weighted transform are derived in such a way that they are only significant in the correct (un-aliased) parts of the transform domain. Consequently high frequencies that would be free to alias in the conventional transform tend to model in the correct part of the weighted transform domain. This improved handling of aliased data may be sufficient to remove or reduce the level of interpolation that would be required by a conventional transform.

In Radon Multiple Attenuation, two velocity fields are required:

- An estimate of the stacking velocity field, $V_s$.
- A maximum velocity for multiple attenuation, $V_m$. This is usually a percentage of $V_s$.

CMP gather data are conditioned prior to the transform. Typically the gathers are moveout corrected with velocity $V_{s,}$ which ideally results in flattened primary reflections and under corrected multiples. For convenience we refer to over-corrected data as having negative dip (decreasing time with increasing offset), under-corrected data as having positive dip (increasing time with increasing offset) and flat data as having no discernible change in time with offset. The amplitudes may also be preconditioned, for example by using a reversible AGC.

The data are then transformed into the tau-p (Radon) domain using a parabolic Radon transform. After hyperbolic normal-moveout (or higher-order moveout correction), residual moveout has an approximately parabolic shape and hence a parabolic Radon transform is appropriate.

The range of moveouts to transform, measured in ms at a reference offset ($X_{ref}$), is chosen to cover the range of both primary and multiple energy. Following this, parts of tau-p domain representing primary energy are zeroed by application of a mute. For this purpose ‘primary energy’ is usually assumed to be any data with a velocity faster than $V_m$. This allows for time-variance in the separation of primary and multiple events. $V_m$ does not need to be the actual velocity of the multiples but rather a velocity that is as fast as or faster than multiples of interest while being slower than the primary velocity. Primary energy is protected at late times by imposing a minimum moveout (p) value on the mute. Note that for some deep water datasets, the mute may be safely defined by use of the minimum p value alone, without reference to $V_m$. The boundary between the zeroed and preserved regions is tapered in the p direction.

Inverse tau-p transform and removal of the pre-transform conditioning produces a model of the multiple energy. This is subtracted from the original data to produce the multiple-attenuated output.

Parameter values:

| | |
|---|---|
| Pre-transform conditioning | : NMO with primary velocity, 252ms AGC |
| Reference offset($X_{ref}$) | :4060m |
| Moveouts ($\Delta t$ ) at the reference offset ($X_{ref}$ ): | |
| Minimum moveout (i.e. for the first p-trace) | : -750 ms |
| Maximum moveout (i.e. for the last p-trace) | : 2750 ms |
| Number of p-traces generated | : 700 |
| Frequency range of multiple model | : 0-125 Hertz |
| Multiple Mute Velocity ($V_m$) | : 91% of the primary velocity field |
| Mute minimum moveout limit | : 250 ms |
| Mute taper (p direction) | : 32 ms |

Note: Moveouts used in making intermediate p-traces were linearly interpolated between the minimum and maximum moveouts.

## *2.16 3D XLine Grid*

Antares Xline 3D grid was applied to all three surveys prior to the matching and prestack regularization.

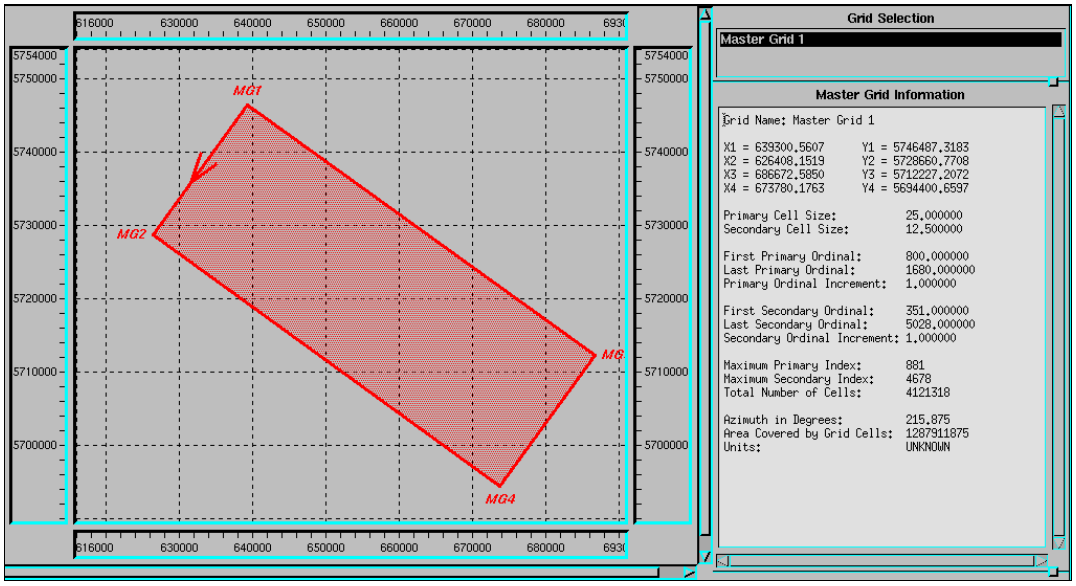


**Figure 2: 3D Xline Grid**

## 2.17 Survey Matching

Where datasets from multiple surveys are to be merged together it is first necessary to compare the datasets to derive a filter to match the datasets in terms of their phase and amplitude spectra, amplitude level and event timing. This comparison requires that the two surveys (the source and target surveys) overlap each other so that coincident trace locations can be extracted. A cross-equalisation filter is derived that performs the matching of the adjunct data to the primary data. Either a single or space-variant cross-equalisation filter can be designed.

### 2.17.1 Cross-equalisation spectral analysis

Autocorrelations are generated on all coincident traces over a time window around the main zone of interest. The coincident adjunct- and primary-traces are also cross correlated over the same time window. The peaks of the cross correlation traces are time aligned and then either spatially averaged or summed together depending on whether a single or space-variant cross-equalisation filter is required. The time shifts required to align the individual cross correlation traces indicate the timing differences between the adjunct and primary datasets. QC plots can be made to show how these time shift values vary over the overlap area and anomalous traces discarded prior to the averaging.
The averaged or summed autocorrelation and cross correlation trace provides spectral estimates that are used to generate the cross-equalisation filter or filters.

### 2.17.2 Cross-equalisation filter design

The cross-equalisation filter design process uses either a polynomial or least squares fitting method to derive a filter that matches the adjunct to the primary over a defined frequency range. The user may optionally taper the autocorrelation and cross correlation functions prior to filter design.

### 2.17.3 Phase-only and fixed-phase equivalents

Having derived a filter it is sometimes preferable to apply the phase-only equivalent of the filter or alternatively apply a fixed phase rotation to the data that simulates the effect of the cross-equalisation filter over the dominant bandwidth. Both of these options can be achieved by further manipulation of the cross-equalisation filters derived in the previous stage.

### 2.17.4 Amplitude level matching

If the adjunct and primary datasets have been processed through similar processing sequences then it is likely that a single fixed scalar is all that's required to bring the amplitude levels together. If however, the datasets have been processed independently then it may be necessary to perform a time-variant amplitude analysis, on the coincident traces, and derive a single time-variant scalar to match the two.

Parameter Values:

| | |
|---|---|
| Adjunct survey name | : Casino M3D |
| Primary survey name | : Antares M3D |
| Cross-equalisation analysis window | : 500-2000 ms |
| Matching filter type | : Amplitude/Fixed phase rotation |
| Fixed phase rotation | : -64deg |
| Time shift applied to source data | : 0ms |
| Amplitude scalar type | : Simple |
| Amplitude scalar | : 2.64 |

Parameter Values:

| | |
|---|---|
| Adjunct survey name | : Minerva M3D |
| Primary survey name | : Antares M3D |
| Cross-equalisation analysis window | : 500-2000 ms |
| Matching filter type | : Amplitude/Fixed phase rotation |
| Fixed phase rotation | : -64deg |
| Time shift applied to source data | : 0ms |
| Amplitude scalar type | : Simple |
| Amplitude scalar | : 0.67 |

## *2.18 Target Migration Velocity Analysis*

Velocity analysis was performed using **WesternGeco's** Interactive Velocity Processing (INVA) package.

NMO-corrected gathers are then produced to check the validity of the picks and any necessary changes made before the velocity field is output.

Parameter Values:

| | |
|---|---|
| Analysis Spacing | : 1km |
| Number of CMPs per Analysis (MVF Stack) | : 15 |
| Number of CMPs per Analysis (Semblance Display) | : 3 |

## *2.19 Survey Coordinate Transformation*

The Minerva survey coordinates where transformed to the same spheroid as the Minerva and Antares survey coordinates.

Parameter Values:

Transformation :- ANZ to WGS84

X_Shift = -116
Y_Shift = -50.5
Z_Shift = 141.7
X_Rotation = 0.0000011150715
Y_Rotation = 0.0000018907734
Z_Rotation = 0.0000016677591
Scale Factor = 0.0983
Rotation Type = Position Vector

Note:- WGS84 is equivalent to GDA94 +/- 1m

## *2.20 3D Prestack Fold Interpolation and Regularization*

This process is a seismic interpolation and regularization tool for pre-stack 3D data that are irregularly sampled in space. It provides an improved method of regularizing 3D fold of coverage relative to the conventional flex binning approach of copy and move employed to fill gaps in coverage. The process also allows for the prestack regularization of traces to move them (via interpolation) to their respective cell-centre positions.

In partial regularization, the original data remain unaltered and traces are only interpolated to fill empty cells. Such partial regularisation can be useful prior to Prestack Time or Depth Migration where irregular subsurface fold can result in undesired amplitude variations.
Each interpolated output trace was calculated from a cluster of nearby input traces using adaptive interpolation. An optional dip map was computed to guide the interpolation and thus enable it to handle steeply dipping events. At each sample, the data were scanned over a range of dips to determine the local dominant dip. The dip-search was accomplished by computing the non-normalised semblance (correlation) between nearby traces for the range of dips of interest; peaks in the semblance indicate local dominant dips.
The interpolated trace was then constructed by a weighted sum of input traces along the local dominant dip for each output sample.
The interpolation process was performed on common offset planes using a time-space (t-x) sinc interpolation that adapted to the local input cluster density and dominant dip.
Limits were set for the maximum number of traces in an output cell. To accomplish this, redundancy editing was applied and the trace (or traces) closest to the cell centre were kept.

Parameter Values:

| | |
|---|---|
| Operation Mode | : Infill holes / Trace Regularization |
| Maximum no. of traces in output cell | : 1 |
| Sinc Interpolation length (inline x crossline) | : 13x17 |
| Number of Dip Scans | : 11 |
| Dip Range | : -1ms/trace to +1ms/trace |
| Correlation Width | : 13 traces |
| Correlation Length | : 104ms |

## *2.21 Pre-Stack Time Migration*

The Kirchhoff Time Migration Seismic Function Module (SFM) performs seismic time migration using the Kirchhoff summation method. The migrated image is constructed by summing weighted amplitudes along diffraction curves or curved surfaces for the 3D case. These diffraction curves are determined by two-way travel times from the surface to subsurface scatterers that are computed from the user-supplied velocity field. In prestack mode, migration is performed on common offset volumes for 3D data.

Theoretical Basis

Kirchhoff migration is based on Green's theorem, a mathematical equation that states a relationship between the observations of a wave field on a closed surface and the wave field at any point inside that surface (see Schneider, W.A., 1978). The name of Gustav Kirchhoff is associated with the method because of his work in 1882 on optical diffraction. The formula for migration that is derived from Green's theorem has the form of an integral (or a summation in the case of discretely sampled data) over observations made on the surface of the earth. The migrated image calculated by that summation represents the acoustic reflectance throughout a section of the earth beneath the surface observations.

Key parameters to the migration process are the Maximum Dip Filter Angle and Spatial Anti-aliasing factors. Kirchhoff Migration typically provides a better migration solution, compared with other time migration algorithms, when the velocities vary both laterally and temporally. One feature of the WesternGeco's Kirchhoff Migration is the ability to define an output location, line or volume independently of the input data. This allows the user to target the output of selected lines or locations that are fully 3D migrated without the associated time/cost of migrating the whole volume. This target output option is particularly useful when processing 3D pre-stack as it allows the generation of targeted velocity analyses prior to running the full migration. Under such circumstances, the process does not waste time migrating those input traces that do not contribute to the output profile.

Prestack migration is achieved by migrating the sorted common-offset panels into individual zero-offset panels. During migration the traces are effectively NMO-corrected; however, inverse NMO using the migration velocity is typically applied prior to output of the data. This allows a final velocity analyses and moveout to be performed on the data prior to stacking it.

Parameter Values:

| Time (ms) | Max Dip Limit (degrees) |
|---|---|
| 0 | 60 |
| 1000 | 60 |

## *2.22 Final Migration Velocity Analysis*

Velocity analysis was performed using **WesternGeco's** Interactive Velocity Processing (INVA) package.

NMO-corrected gathers are then produced to check the validity of the picks and any necessary changes made before the velocity field is output.

Parameter Values:

| | |
|---|---|
| Analysis Spacing | : 500 m |
| Number of CMPs per Analysis (MVF Stack) | : 15 |
| Number of CMPs per Analysis (Semblance Display) | : 3 |

## *2.23 Residual Radon Multiple Attenuation*

This pass of Radon Multiple Attenuation was used to attenuate residual multiple energy. The improved velocity control available from performing the velocity analysis after migration, allowed a more severe mute to be applied than that used in the first pass of Radon Multiple Attenuation.

Parameter values:

| | |
|---|---|
| Pre-transform conditioning | : NMO with primary velocity, 252ms AGC |
| Reference offset($X_{ref}$) | :4060m |
| Moveouts ($\Delta t$ ) at the reference offset ($X_{ref}$ ): | |
| Minimum moveout (i.e. for the first p-trace) | : -750 ms |
| Maximum moveout (i.e. for the last p-trace) | : -750 ms |
| Number of p-traces generated | : 300 |
| Frequency range of multiple model | : 0-125 Hertz |
| Multiple Mute Velocity ($V_m$) | : 94% of the primary velocity field |
| Mute minimum moveout limit | : 120 ms |
| Mute taper (p direction) | : 32 ms |

Note: Moveouts used in making intermediate p-traces were linearly interpolated between the minimum and maximum moveouts.

## 2.24 Polygon Select

Low Fold areas that contained a lot of migration swirl were removed from stack.

| SL/IL relation | Sail line = Xline |
|---|---|
| xline | Inline |
| 947 | 4520 |
| 947 | 3363 |
| 996 | 3363 |
| 996 | 595 |
| 1265 | 595 |
| 1265 | 2138 |
| 1380 | 2138 |
| 1380 | 3038 |
| 1328 | 3469 |
| 1261 | 3440 |
| 1261 | 3520 |
| 1435 | 3880 |
| 1435 | 4520 |

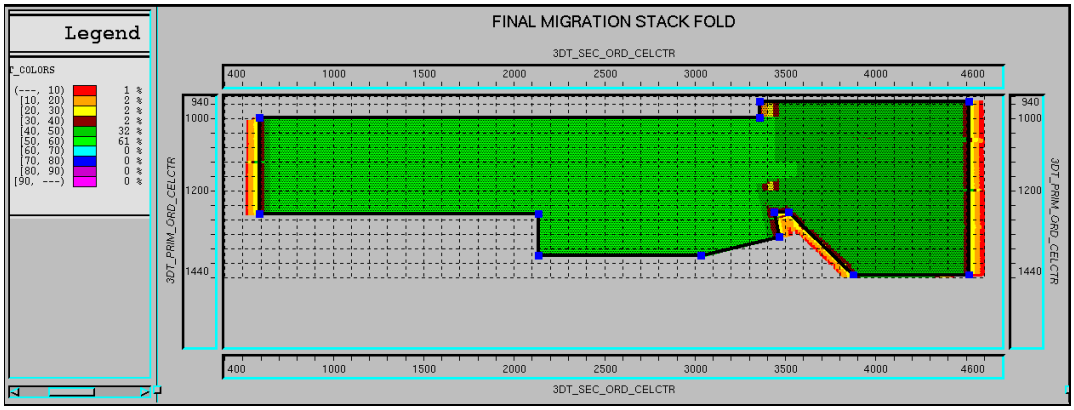


**Figure 3: Fold of Coverage with polygon**

## 2.25 Residual Moveout (CIP/RMO_FIT)

CIP estimates the times of seismic events in prestack migrated common image point gathers, referred to as CIP gathers. The time of each event is determined automatically by performing a flat linear semblance on the CIP, and then picking the highest semblance values.

Once events are identified, the SFM performs various parabolic and linear scans.
The moveout curve corresponding to the maximum semblance (whether linear or parabolic) is retained by the SFM at each time event.

A moveout correction is then applied to the event using the estimated curve followed by a trim static like procedure to remove the non-linear or non-parabolic residual moveout.

This was applied to one set of gathers for producing an aligned set of near, mid and far angle/offset stacks.

Parameter values:

CIP Pick:
Analysis Locations :125x125m

| | |
|---|---|
| Residual Moveout Fit: | |
| Iline/Xline Smoothing | : 250m |
| Time Smoothing | : 250ms |
| Time Cutoff | : 3200ms |

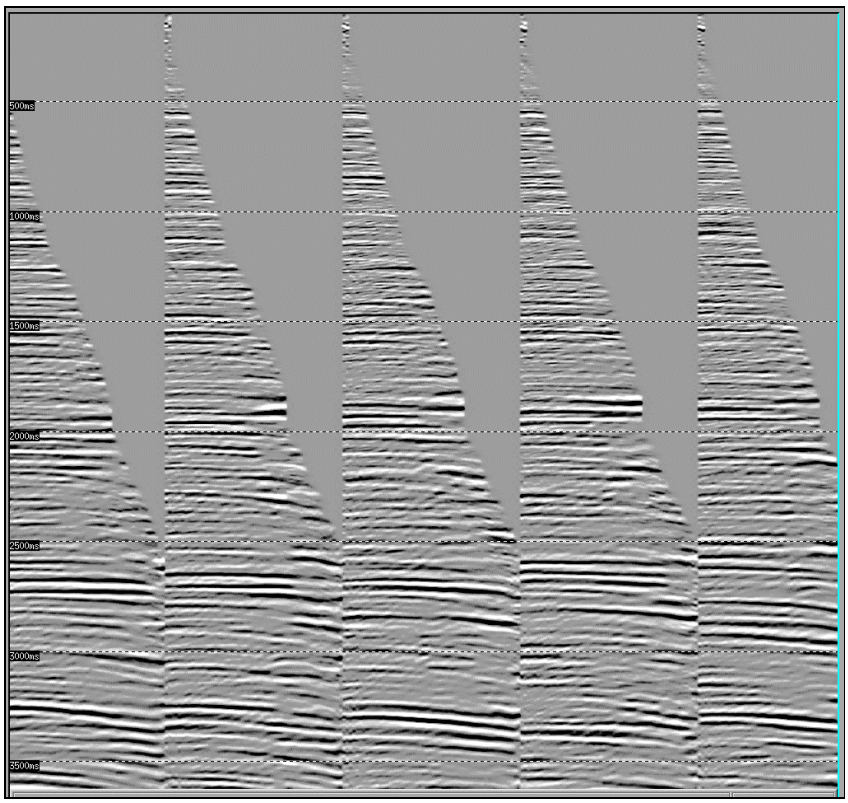


**Figure 4: Residual Radon Selected CMPs**

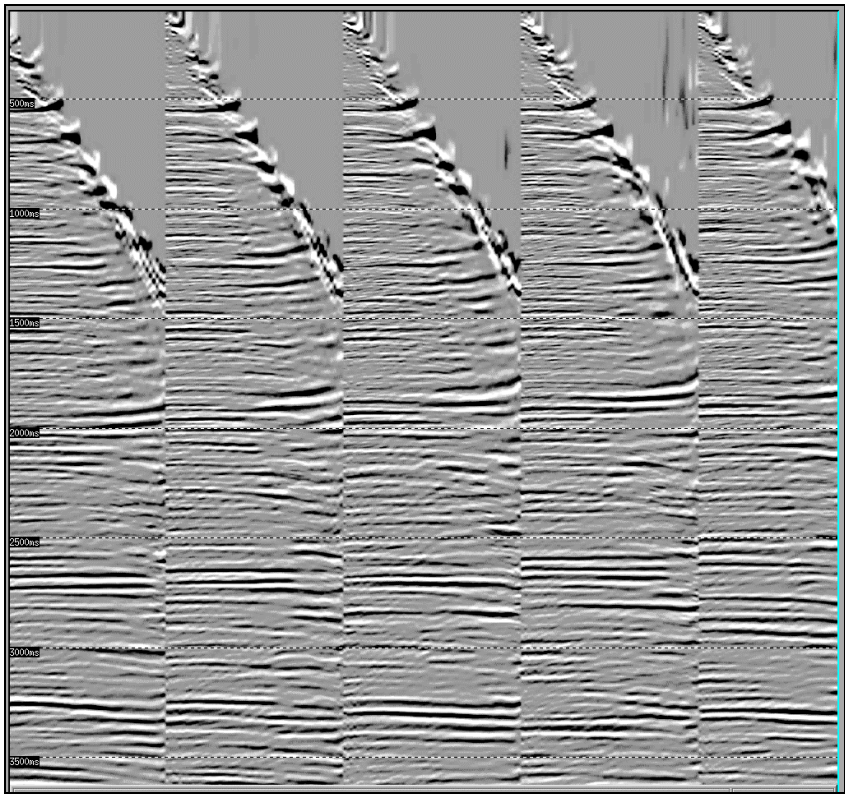


**Figure 5: Residual Radon Selected CMPs with the CIP RMO applied**

## *2.26 Angle Stack*

The velocity functions used to derive the angle mutes were calculated from the smoothed final stacking velocity field. The mutes were calculated using bending rays, to compensate for refraction, with interval velocities calculated using Dix approximation. The resulting velocity function was finally modified by a Least Squares fit to prevent oscillations in interval velocities causing unstable mute patterns.

The 3 Angle stack volumes generated at the request of **Woodside** were:

- Near: 05 – 16 degrees
- Mid: 16 – 27 degrees
- Far: 27 – 38 degrees
- Full 00 – 35 degrees

For the Near, Mid and Far stacks the angle mute was kept constant at the time that the 38degree angle cut the maximum offset.

The traces within each angle-muted gather are stacked to form a single output trace. The resultant trace is normalized sample by sample using the following function:

$$s(t) = \frac{1}{w(t)}$$

where: $w(t)$ is the summed weight function for a given output trace

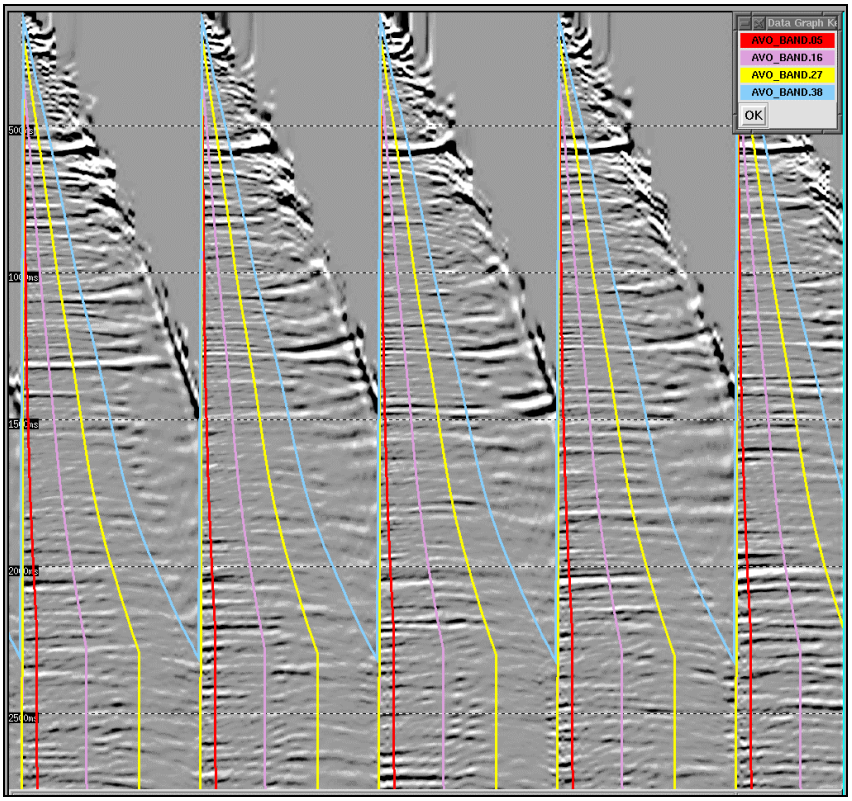


**Figure 6: Angles on Select CMPs**

## *2.27 TVF*

A zero-phase TVF (Time Variant Filter) was applied to the angle stacks so the amplitude spectrum was consistent from near to far . The filter pass bands were described by low- and high-cut frequencies and associated dB/octave cutoff slopes. The specified cutoff frequencies are located at the half-power (-3 dB in amplitude) response points and the slopes at these frequencies are equal to the respective dB/octave values. The slope is an approximate cosine squared function in the amplitude domain. The filters were normalized so that the output amplitudes were the same as the input amplitudes for frequency components within the passband.

Parameter values:

| Filter Centre Time (ms) | Low-cut Frequency (Hz) | Low-cut Slope (dB/octave) | High-cut Frequency (Hz) | High-cut Slope (dB/octave) |
|---|---|---|---|---|
| 4 | N/A | N/A | 80 | 72 |
| 300 | | | 70 | 72 |
| 800 | | | 60 | 72 |
| 1800 | | | 35 | 36 |
| 2800 | | | 25 | 36 |

Note: The times are those at the centre of the filter where the full effect of the filter is attained
The first filter was applied from the beginning of the trace to the first filter centre time
Intermediate filters were linearly tapered and blended with the preceding and succeeding filter between the filter centre times
The last filter was applied from the last filter centre time to the end of the data

## *2.28 AVO Attribute Trace Generation*

In certain depositional settings, the amplitude variation dependent on offset between source and receiver can provide an important clue to the presence of hydrocarbons. The reflection coefficient for an incident plane P-wave can increase or decrease (and even change polarity) with reflection angle, depending on changes in elastic parameters across a reflecting boundary. Conventional CMP stacking suppresses this information because the amplitude of each event in the stack represents an average over all offsets. Consequently, reflection character, event amplitude and continuity on conventional CMP stacks can differ from a zero-offset recorded section.

Several methods exist which allow seismic traces to be generated that, unlike conventionally stacked traces, exploit information about the dependence of amplitude on reflection angle.

In AVO Attribute Trace Generation corresponding time-samples of traces in a NMO-corrected CMP gather are used to fit a straight line to amplitude versus the reflection angle - more strictly, amplitude versus $\sin^2(\Phi)$, where $\Phi$ is the reflection angle. (Reflection angle is computed from offset-time by either a straight-ray or a bending-ray approximation, with velocities derived from the rms velocities). The result is a slope and intercept value for a given two-way time. Repeating the process for all times generates the attribute traces referred to as the 'gradient stack' and 'intercept stack', respectively. These new stacks allow estimates of:

Local changes in P-wave impedance (the intercept trace);
Contrasts in S-wave impedance (the difference between the intercept and slope traces, under certain assumptions);
Variations in Poisson's ratio across interfaces (the sum of the intercept and slope traces, under a different set of assumptions).

The AVO attribute stacks aid in detailed lithologic and stratigraphic analysis and complement structural information obtained from a conventional CMP-stack section. In particular, the P-wave stack is a better approximation to the zero-offset section than the CMP stack and is better suited, therefore, in estimating $V_p$; the gradient stack retains the algebraic sign information of the gradient and can be used to estimate $V_s$; the S-wave stack approximates the zero-offset S-wave section with travel times governed by the P-wave velocities and can be used to correlate with the P-wave stack to identify lithology; and the product stack restricts the gradient to be positive when the reflection strength increases with offset and negative otherwise.

To remain consistent with general industry practice, the intercept has a polarity convention where a positive increase in reflection coefficient is represented by a positive number.

Parameter Values:

Angle Computation :5-30 degrees

Attribute stacks created : P-wave Stack
Gradient Stack

# *3.0 Personnel*

Key individuals involved in the project were:

For **Woodside**

| | |
|---|---|
| Robert Eliott-Lockhart | Representative |

For **WesternGeco**

| | |
|---|---|
| King Seong Tan | Processing Supervisor |
| Monica Wurfel | Project Leader |
| Richard Bisley | GeoSupport |

# 4.0 Appendices

## 4.1 Acquisition Parameters

### 4.1.1 Acquisition Parameters Antares 3D Marine Seismic Survey

| **General Information** | |
|---|---|
| Client | Woodside Energy Ltd |
| Contractor | PGS |
| Vessel | M/V ORIENT EXPLORER |
| Survey Name | Antares 3D Marine Seismic Survey |
| Type of Survey 3D seismic | 3D seismic |
| Mode of Shooting | 4 streamers / dual source / flip-flop |

| **Survey** | |
|---|---|
| Total Proposed Full-Fold | Area 210.24l |
| Total Full-Fold CDP Kilometres | 8,409.6 from pre-plot co-ordinates |
| Full-Fold Sail Line Kilometres | 1,051.2 from pre-plot line co-ordinates |
| Number of Sail Lines | 33 |
| Geographical Sail Line Orientation | 125° / 305° |

| **Recording** | |
|---|---|
| Recording Instruments | Syntrak – 960-24 |
| Recording System | Syntrak – 960 - 24 |
| Dual Recording | Yes |
| Recording Media | Imation and Emtec 3590 cartridges/ASCII/TAR |
| Recording Format | SEG-D 8058 |
| Record Length | 6.0 s |
| Sample Rate | 2 ms |
| Low Cut Filter/Slope | 3 Hz at 12dB/Oct (out) |
| High Cut Filter/Slope | 206 Hz at 276 dB/Oct |
| Seismic Channels | 1,296 (324 per streamer) |
| Dual Recording/Tape Copy | No – tape copies produced off-line |

| **Streamer** | |
|---|---|
| Streamer Type | Syntrak digital telemetric streamer |
| Number of Streamers | 4 |
| Active Streamer Length | 4050 m/streamer |
| Active Groups | 324 per streamer total 1296 groups |
| Group Interval | 12.5 m |
| Group Length | 16.12 m (12 phones/group) |
| Hydrophone | Teledyne T2 |
| Hydrophone Sensitivity | 20V/Bar at 10 Hz (rated) |
| Hydrophone Sensitivity | 20.8 to 21.7 V/bar tested |
| Towing Depth | 7.5 m ± 1.0 m |
| Streamer Separation | 100 m between each streamer |
| Total Streamer Spread | 300 m lateral spread (streamer 1 to 4) |
| Cable-Levellers | 17 Digicourse depth controllers/streamer (extra compass at head and tail-end) Digicourse 5011. |

| **Energy Source** | |
|---|---|
| Energy Source | Bolt airguns |
| Operating Pressure | 1,800 psi |
| Volume | 2,500 cu.in per energy source |
| Number of Sub Array Strings | 3 per energy source |

| | |
|---|---|
| Synchronisation Tolerance | ±1 ms (90% within 1 ms 10% within 1.5 ms) |
| Source Depth | 6 m ± 0.5 m |
| Energy Source Separation | 50 m (centre-to-centre) |
| Source Array Length | 14 m |
| Source Array Width | 10 m |
| Compressors | 4 |
| Near Field Recording | Yes |

| **Navigation and Positioning** | | |
|---|---|---|
| Primary Navigation | StarFix Spot dGPS | SkyFix Spot dGPS |
| RTCM Delivery System | Optus Sport | Optus Spot, Inmarsat POR |
| Reference Stations | Melbourne 220 km | Melbourne 200 km |
| | Adelaide 550 km | Adelaide 520 km |
| | Cobar 840 km | Sydney 920 km |
| | Bathurst 850 km | Brisbane 1,570 km |
| Contractor | Fugro-Survey AS | Thales GeoSolutions |

| **Datums** | |
|---|---|
| Survey Datum | GDA94 |
| Ellipsoid | GRS80 |
| Semi-Major Axis | 6378137 m |
| I/Flattening | 298.257222101 |
| GPS Datum | WGS84 |
| Ellipsoid | WGS84 |
| Semi-Major Axis | 6378137 m |
| I/Flattening | 298.257223563 |
| Geod Height - | 1.6 m (EG96) (Woodside reccom.) |
| | (min. –1.90 m, max. –1.45 m) |

| **Datum Shift/Transformation** | |
|---|---|
| From WGS 84 to GDA94 | |
| EPSG Transformation Code No: | 1150 |
| DX (m) | 0 |
| DY (m) | 0 |
| DZ (m) | 0 |
| Magnetic Variation | 10.9º recommended |
| *Note:- GDA94 is a realisation of WGS84 coincident to within 1.5 m. | |
| This transformation has an accuracy equal to the coincidence figure. | |

| **Map Projection** | |
|---|---|
| Projection | MGA Zone 54 |
| Projection System | Transverse Mercator |
| Central Meridian | 141º east/ zone 54 |
| Scale Factor on Central Meridian | 0.9996 |
| Latitude of Origin | 0º south |
| False Easting | 10,000,000 m |
| False Northing | 500,000 m |

| **Block Boundary** | |
|---|---|
| Northing (Metres) | Easting (Metres) |
| 635788.17 | 5734696.87 |
| 639655.90 | 5740044.83 |
| 667520.90 | 5719892.46 |
| 665226.28 | 5716719.65 |
| 652701.69 | 5722464.78 |

| **3D Grid Specifications** | |
|---|---|
| Number of Sail-Lines | 33 |
| Number of Sub-Surface Lines | 264 |
| Sub-Surface Lines per Sail-Line | 8 |
| Sub-Surface Line Separation | 25 m |
| 3D Bin Length | 18.75 m (acquisition), 6.25 m (processing) |
| 3D Grid Orientation | 125.87°/305.87° |
| Offset Point of Origin | (1,1) 637810.13 E 5742613.35 N/S |
| In-line Cell Length | 6.25 m |
| Cross-Line Cell Width | 25 m |
| CMP Separation | 25 m |
| Shot Interval | 18.75 m |
| CMP Increment | 1 |
| Shot Increment | 1 |
| Area Size | 209 sq km (scale factor not applied) (calculated) |

### *4.1.2 Acquisition Parameters Casino 3D Marine Seismic Survey*

| **General Information** | |
|---|---|
| Client | Strike Oil Nl |
| Contractor | Western Geco |
| Vessel(s) | M/V Geco Resolution |
| Date recorded | October 2001 – November 2001 |
| Survey Name | Casino 3D Marine Seismic Survey |
| Type of Survey 3D seismic | 3D seismic |
| Location | VIC/P44, Victoria, Australia |
| Mode of Shooting | 6 streamers / dual source / flip-flop |

| **Streamer Parameters** | |
|---|---|
| Streamer type | Nessie 4 |
| Number of streamers | 6 |
| Group interval | 12.5m |
| Streamer length | 4000m |
| Streamer depth | 7m |
| Streamer separation | 100m |
| Number of groups per streamer | 320 |

| **Recording** | |
|---|---|
| Recording system | Triacq 1.6c |
| Recording format | SEG-D 8048 |
| Record length | 5.5 sec |
| Sample rate | 2msec |
| Recording filter | (Hi-Cut) 200 Hz@406dB/Oct |
| Recording filter | (Low-Cut) 3 Hz@18 dB/Oct |
| Recording filter delay | 48.07 |
| Recording media | IBM 3590 Cartridge |
| Header System | Geco Extended Header |

| **Source Parameters** | |
|---|---|
| Instrument | TRISOR vers 1.40 |
| Source type | Bolt Airguns |
| Number of sources | 2 |
| Array volume / source | 2x3063 cubic inch (to be confirmed) |
| Operating pressure | 2000 psi |
| Source separation | 50m |
| Shot point interval per shot | 18.75m (37.5m per source) |
| Source depth | 6m |

| | |
|---|---|
| Number of subarrays per source | 2 |
| Number of Airguns per Subarray | 10 |
| Sub array length | 15m |
| Gun Timing Specification | +/- 1.25 sec from T0 |
| Offset c.s-cfg | 143m nominal |

| **Datums** | |
|---|---|
| Survey Datum | WGS84 |
| Ellipsoid | GRS80 |
| Semi-Major Axis | 6378137 m |
| I/Flattening | 298.2572236 |
| GPS Datum | WGS84 |
| Ellipsoid | WGS84 |
| Semi-Major Axis | 6378137 m |
| I/Flattening | 298.2572236 |

| **Map Projection** | |
|---|---|
| Projection | Zone 54 |
| Projection System | Universal Transverse Mercator |
| Central Meridian | 141º east/ zone 54 |
| Scale Factor on Central Meridian | 0.9996 |
| Latitude of Origin | 0º south |
| False Easting | 10,000,000 m |
| False Northing | 500,000 m |

### *4.1.3 Acquisition Parameters Minerva 3D Marine Seismic Survey*

| **General Information** | |
|---|---|
| Client | BHP |
| Contractor | PGS |
| Vessel | M/V ORIENT EXPLORER |
| Survey Name | Minerva 3D Marine Seismic Survey |
| Type of Survey 3D seismic | 3D seismic |
| Mode of Shooting | 4 streamers / dual source / flip-flop |

| **Survey** | |
|---|---|
| Total Proposed Full-Fold | Area 210.24l |
| Total Full-Fold CDP Kilometres | 8,409.6 from pre-plot co-ordinates |
| Full-Fold Sail Line Kilometres | 1,051.2 from pre-plot line co-ordinates |
| Number of Sail Lines | 33 |
| Geographical Sail Line Orientation | 125° / 305° |

| **Recording** | |
|---|---|
| Recording Format | SEG-D 8015 |
| Recording density | 37871 BPI |
| Record Length | 5.0 s |
| **Sample Rate** | 2 ms |
| Low Cut Filter/Slope | 3 Hz at 12dB/Oct (out) |
| High Cut Filter/Slope | 180 Hz at 276 dB/Oct |
| Gain constant | 3 |
| No. of auxiliary channels | 21 |

| **Streamer** | |
|---|---|
| Streamer Type | HSSJ Nessie 3 (Digital) |
| Number of Streamers | 4 |
| Active Streamer Length | 3000 m/streamer |
| Active Groups | 240 per streamer total 960 groups |

| | |
|---|---|
| Group Interval | 12.5 m |
| Group Length | 16.13 m (12 phones/group) |
| Offset | 140m |
| Towing Depth | 8 m ± 1.0 m |
| Streamer Separation | 100 m between each streamer |
| Total Streamer Spread | 300 m lateral spread (streamer 1 to 4) |

| **Energy Source** | |
|---|---|
| Energy Source | Bolt airguns |
| Operating Pressure | 1,800 – 2000 psi |
| Volume | 2,231 cu.in per energy source |
| Shooting mode | Compact source |
| Number of Sub Array Strings | 2 per energy source |
| Source Depth | 6 m ± 0.5 m |
| Shot Point Interval | 18.75 |
| Energy Source Separation | 50 m (centre-to-centre) |
| Source Array Width | 10 m |
| Number of guns per array | 8 |

| **Datums** | |
|---|---|
| Survey Datum | AGD84 |
| Spheroid | ANS |
| Semi-Major Axis | 6378160 m |
| I/Flattening | 298.25 |
| GPS Datum | WGS84 |
| Semi-Major Axis | 6378137 m |
| I/Flattening | 298.257223563 |

| **Datum Shift/Transformation** | |
|---|---|
| From WGS 84 to AGD84 | |
| DX (m) | 116 |
| DY (m) | 50.47 |
| DZ (m) | -141.69 |
| RX(arc sec) | -0.230 |
| RY(arc sec) | -0.390 |
| RZ(arc sec) | -0.344 |
| Scale | -0.098 ppm |
| Magnetic Variation | 10.7º east |

| **Map Projection** | |
|---|---|
| Projection | Zone 54 |
| Projection System | Transverse Mercator (AMG-66) |
| Central Meridian | 141º east/ zone 54 |
| Scale Factor on Central Meridian | 0.9996 |
| Latitude of Origin | 0º south |
| False Easting | 10,000,000 m |
| False Northing | 500,000 m |

## 4.2 Testing Log

### 4.2.1 Amplitude Recovery

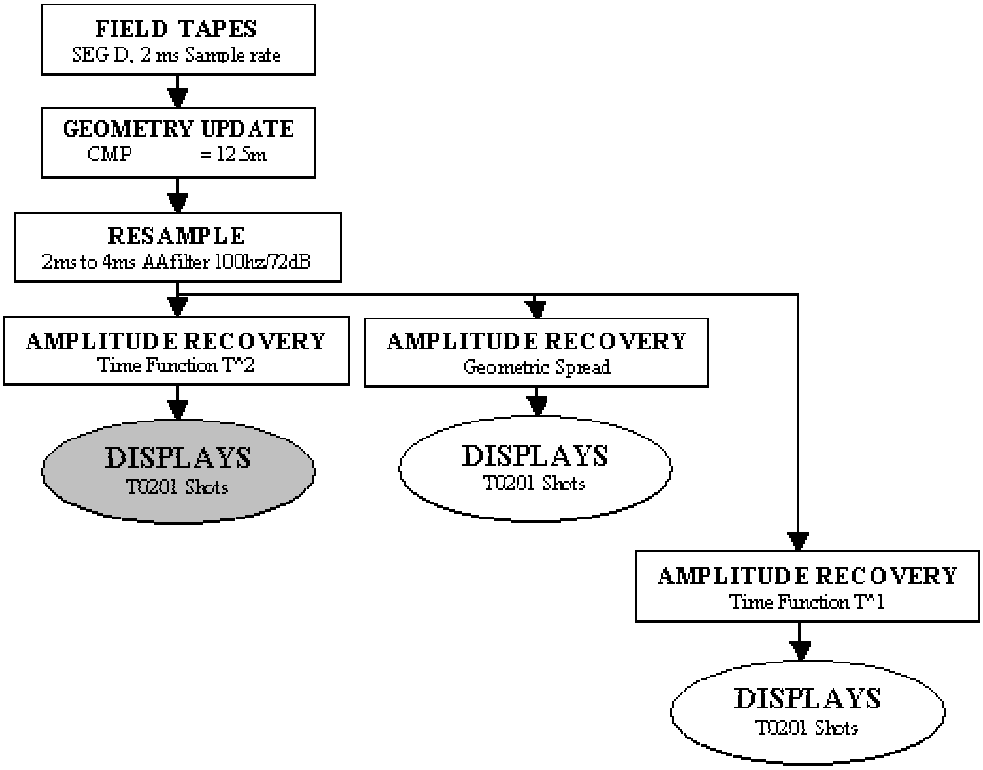


### 4.2.2 Low Cut Filter

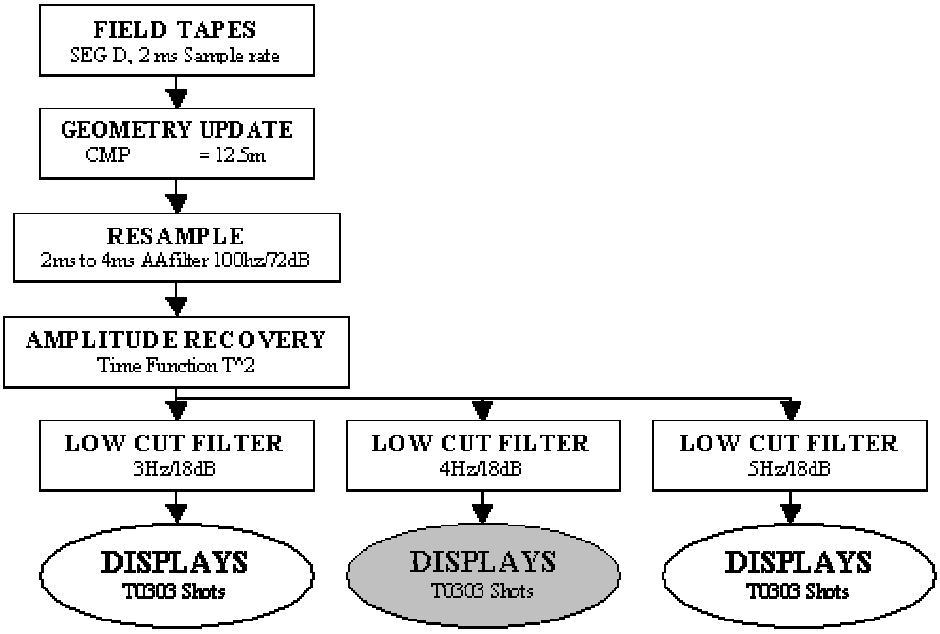

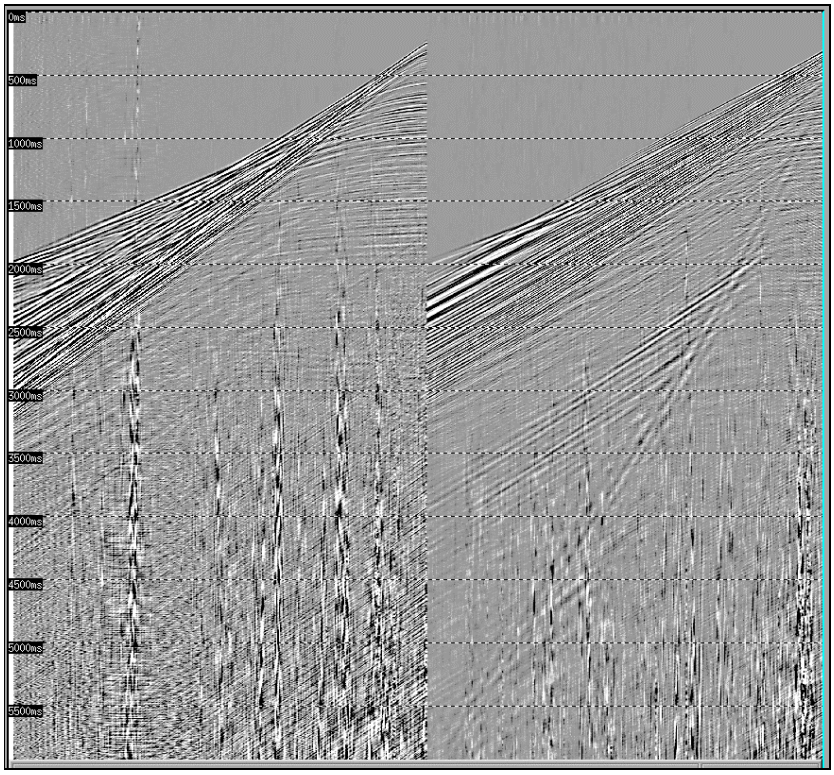


**Figure 7: Raw Shots**

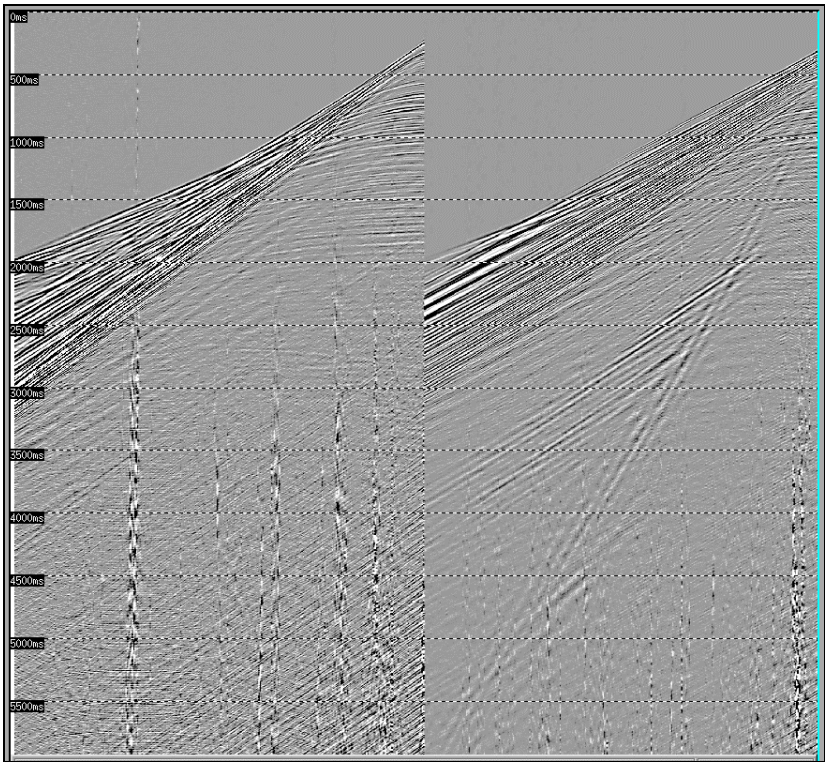


**Figure 8: After Low Cut 4Hz/18db Shots**

### *4.2.3 Swell Noise Attenuation*

Frequency scans were produced to determine the frequency cut-offs for the swell noise attenuation, also a range of thresholds were tested.

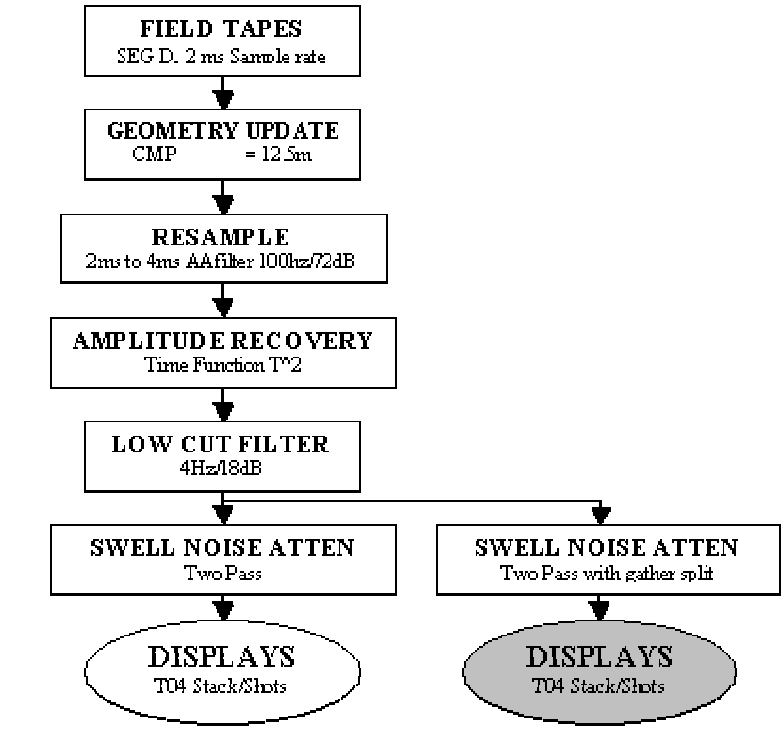


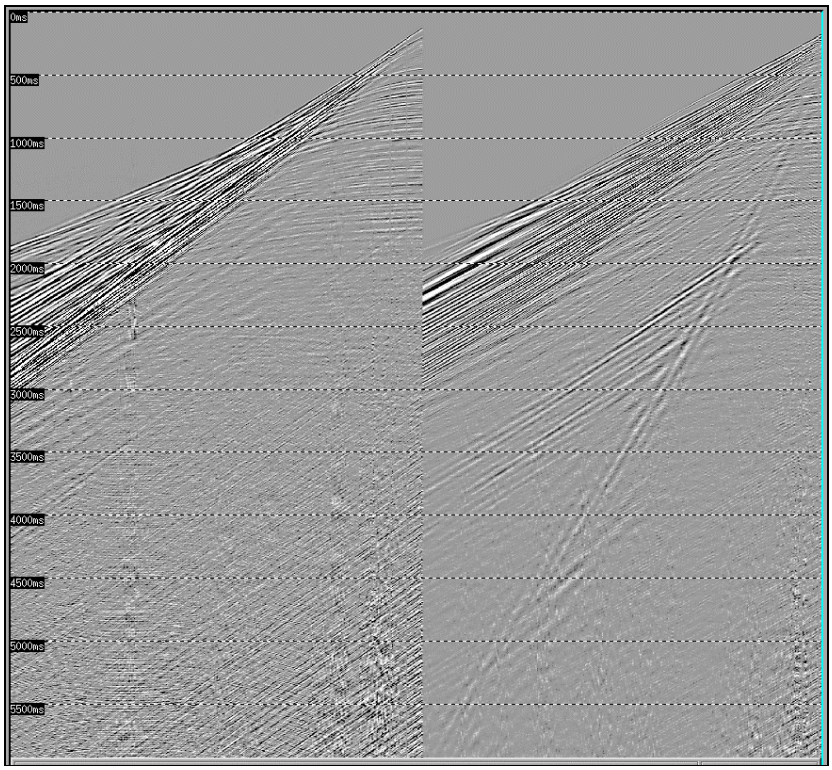


**Figure 9: After Swell Noise Attenuation**

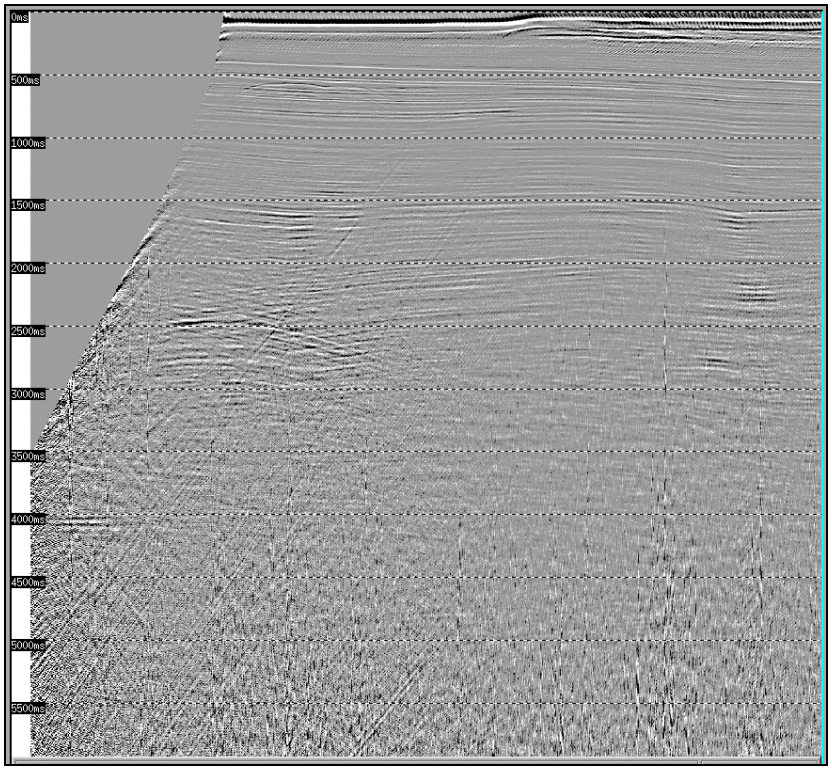


**Figure 10: Brute Stack**

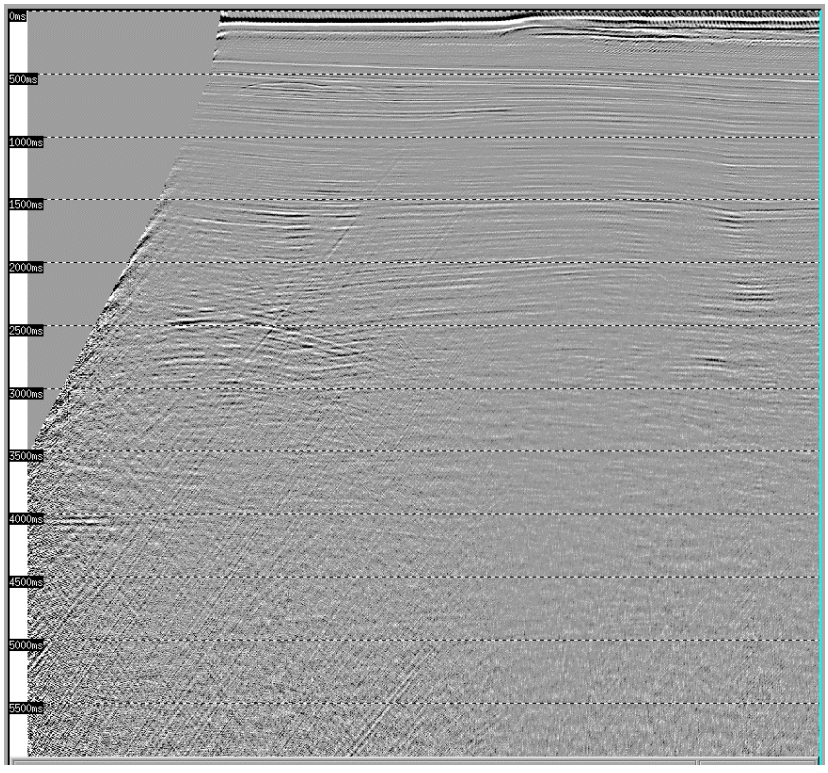


**Figure 11: After Swell Noise attenuation**

### *4.2.4 F-K Dip Filter*

The velocity cuts were estimated from the FK spectrums of several shots.

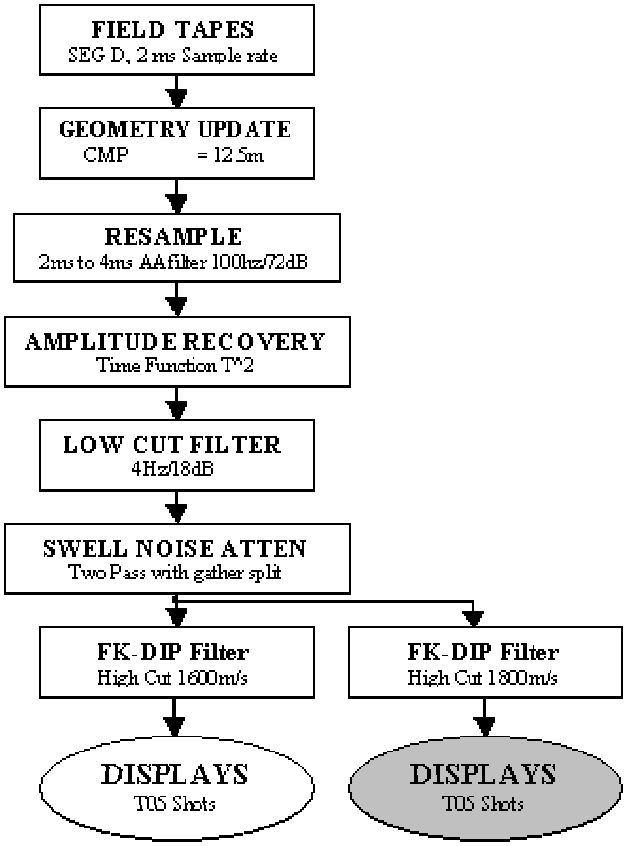


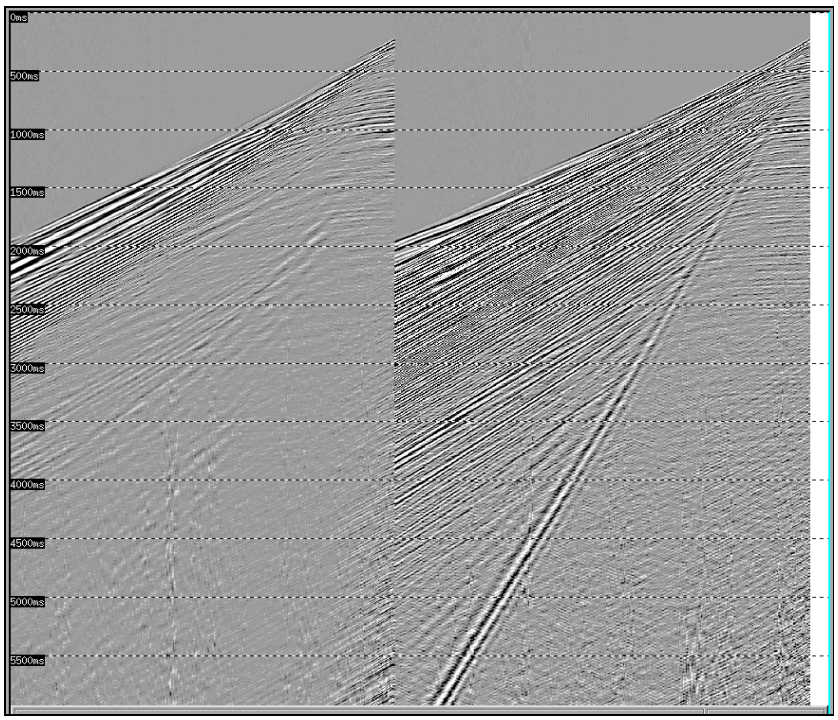


**Figure 12: Mud Roll on Selected shot**

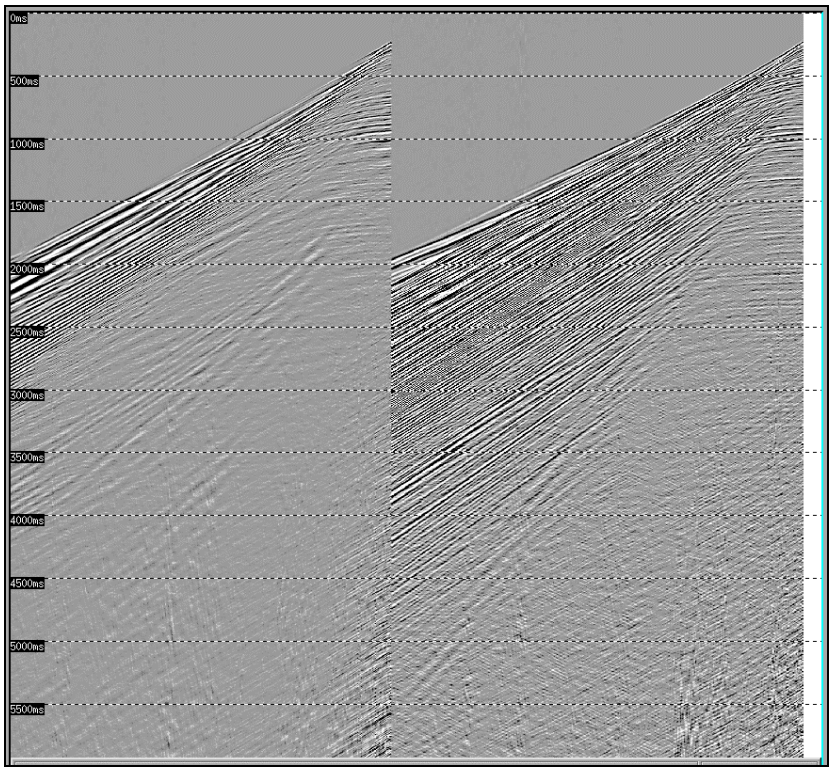


**Figure 13: Selected shots after FK-dip filter**

### *4.2.5 Tau-P linear noise attenuation and Deconvolution*

In the tau-p domain a mild, medium and severe mute were picked and tested to remove the linear noise. Tapering and interpolation were tested to reduce the smearing in the tau-p domain.

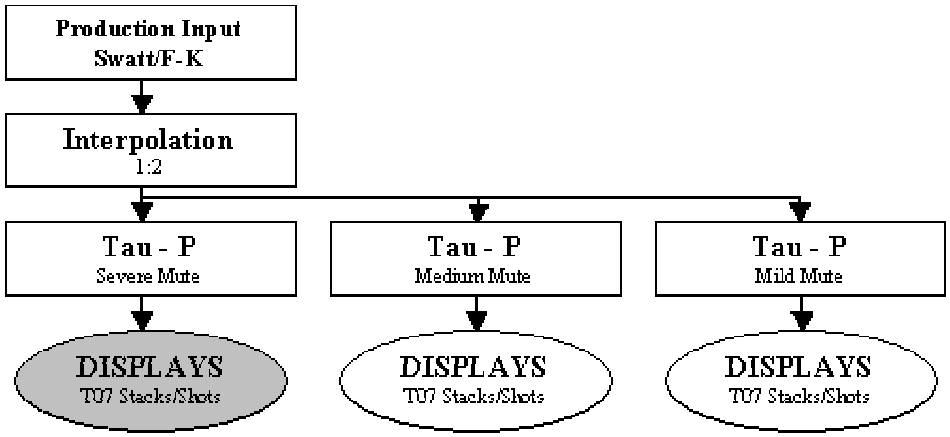

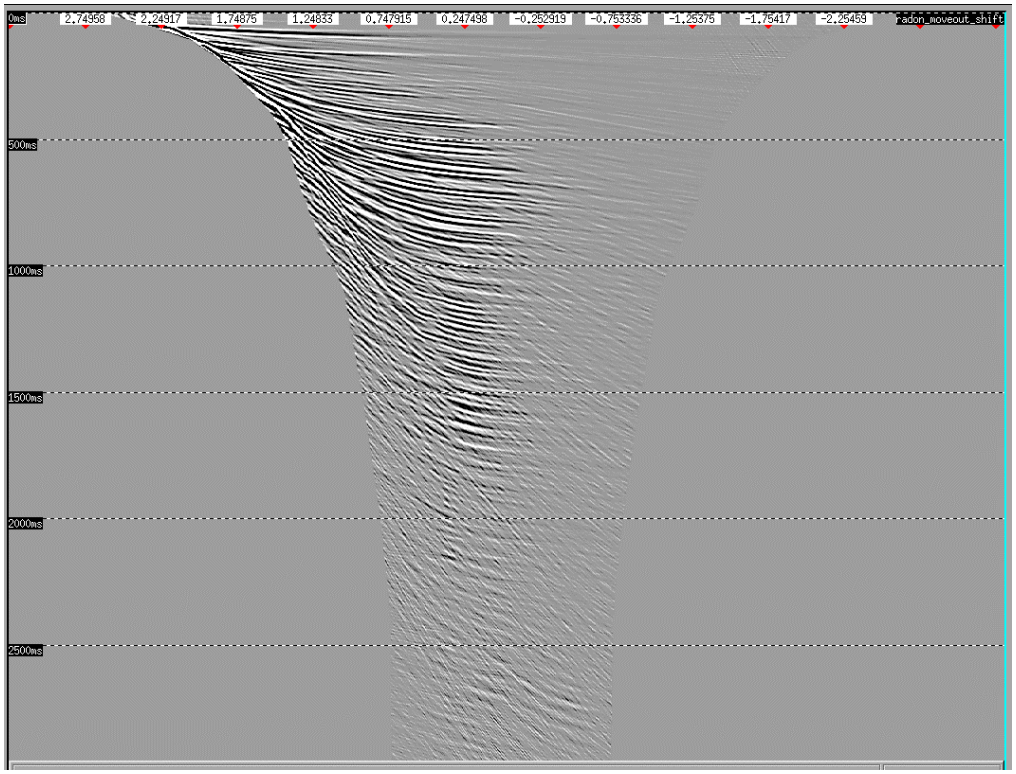


**Figure 14: Example of severe mute applied in the tau-p domain**

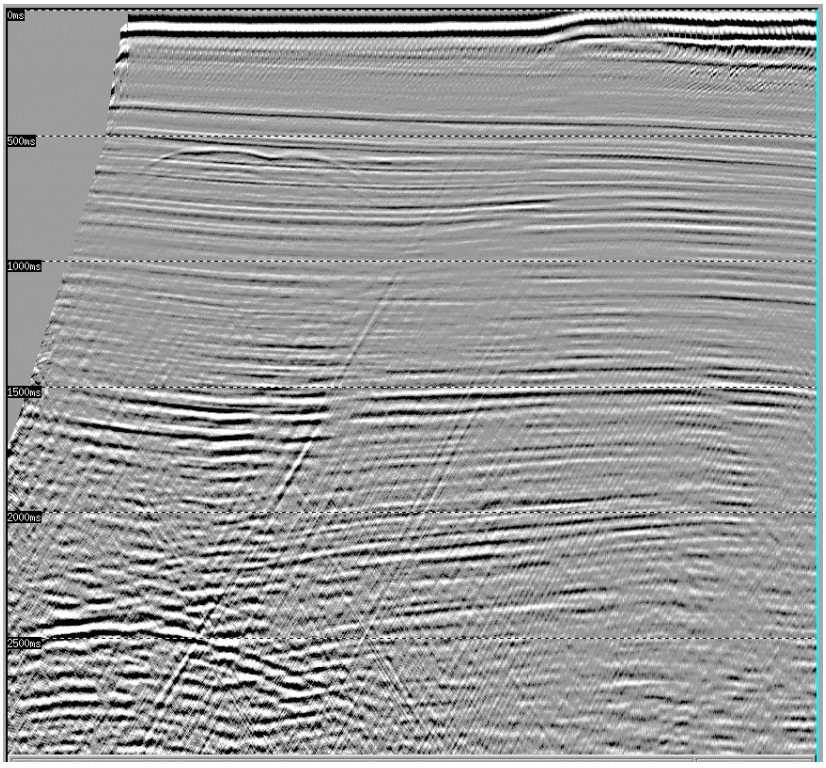


**Figure 15: SWATT and F-K dip filter Stack**

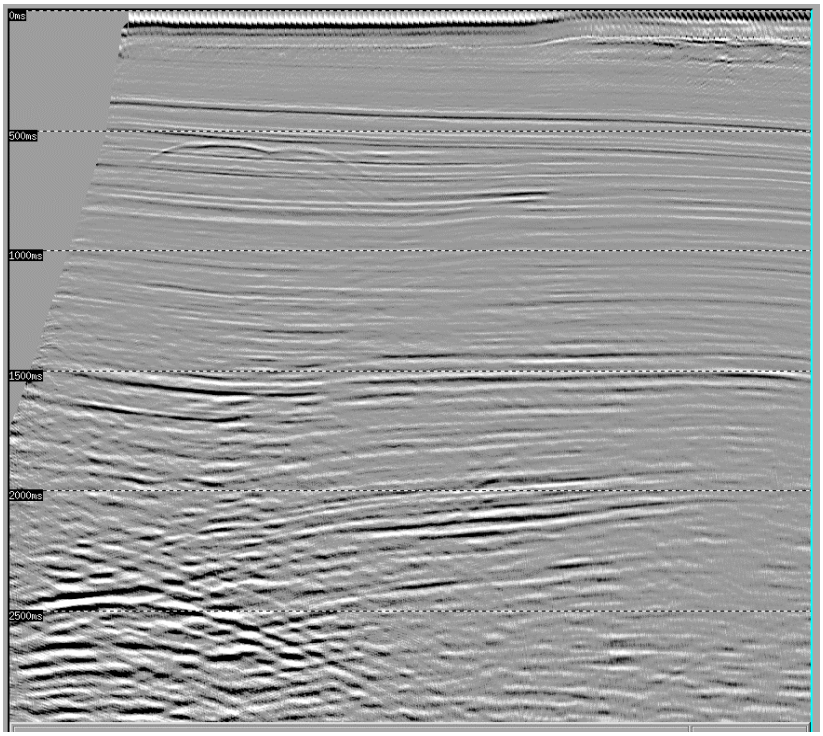


**Figure 16: Stack after Tau-p deconvolution and linear noise mute**

### *4.2.6 Radon demultiple*

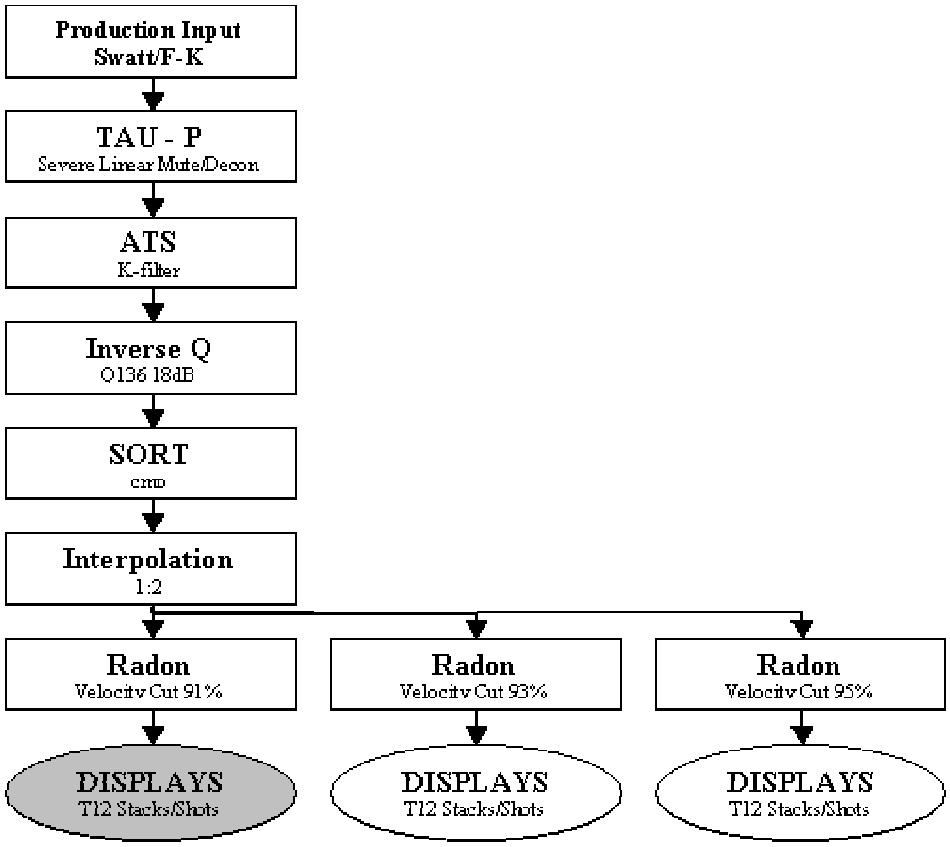

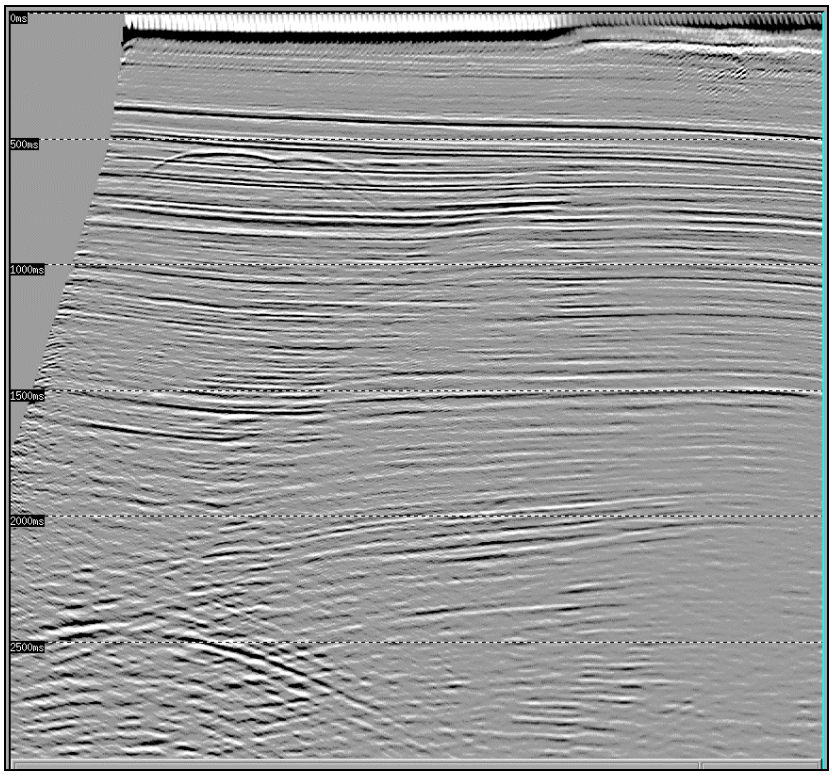


**Figure 17: Stack before Radon**

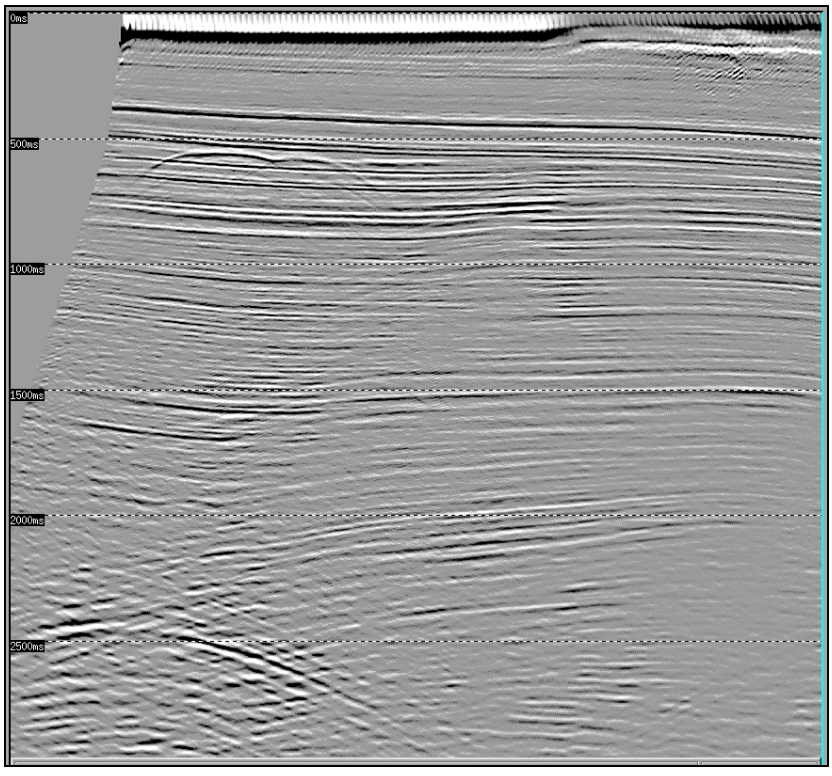


**Figure 18: Stack after Radon**

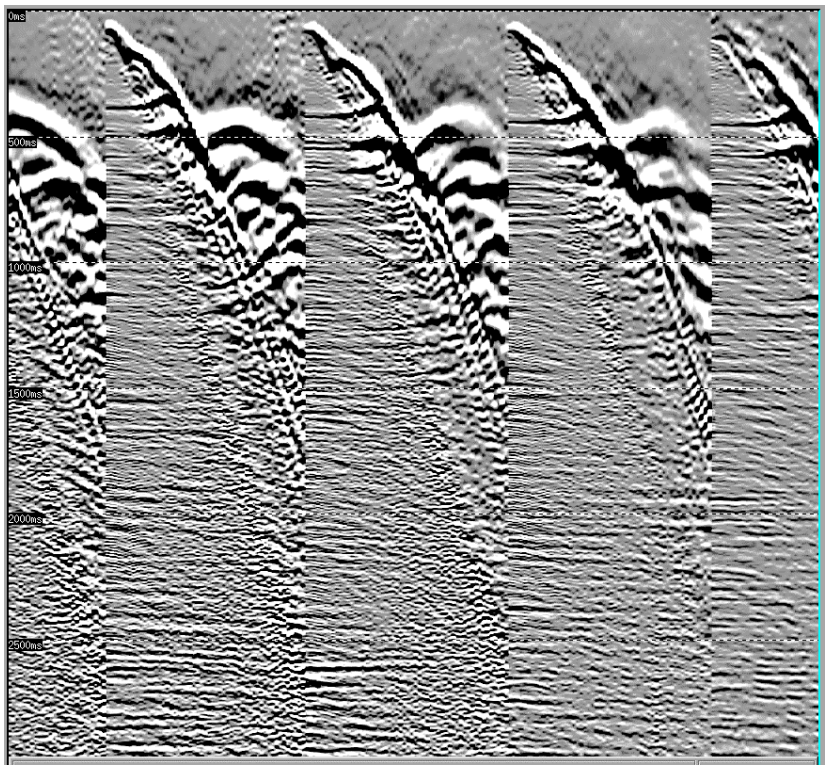


**Figure 19: Selected CMPs before Radon Demultiple**

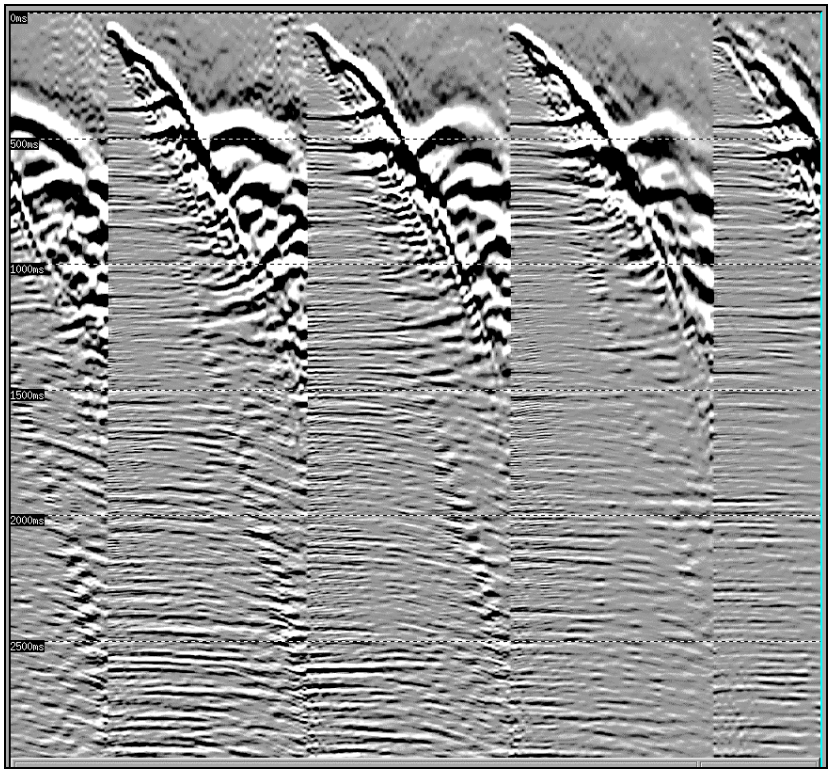


**Figure 20: Selected CMPs after Radon demultiple**

### *4.2.7 Prestack regularization*

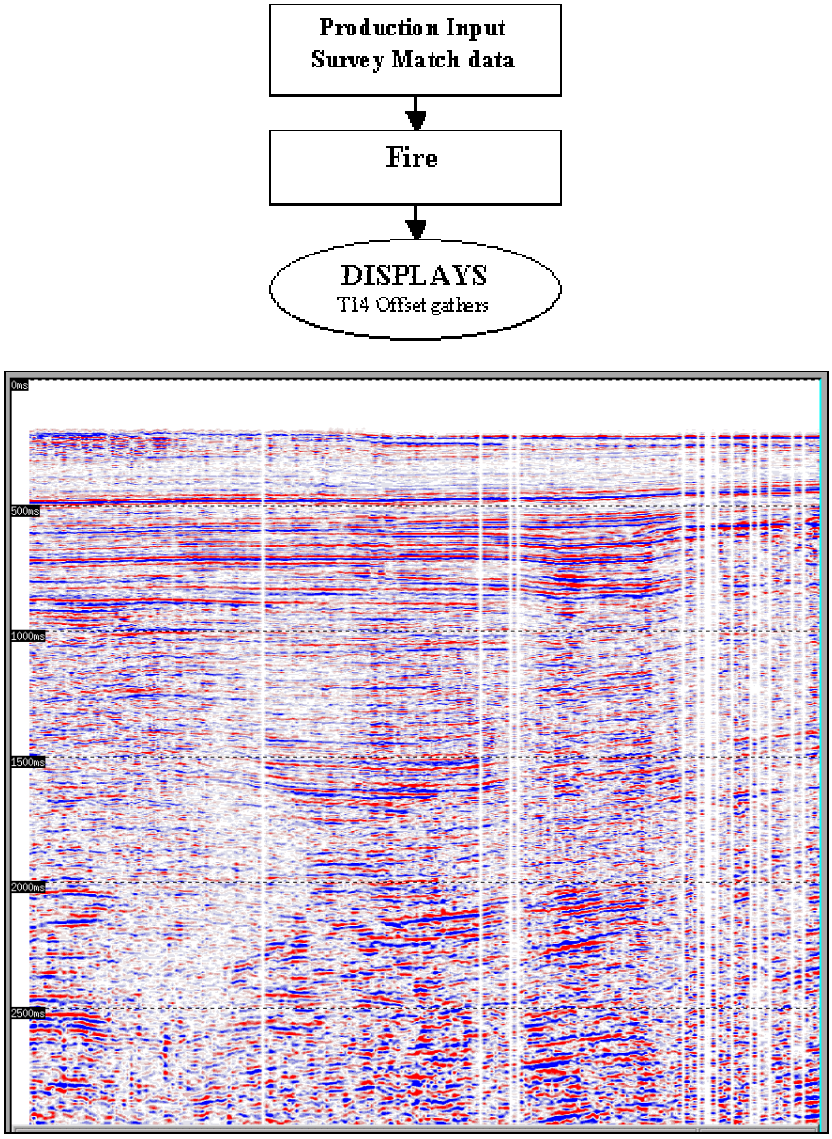


**Figure 21: Single offset over the merge area before regularisation**

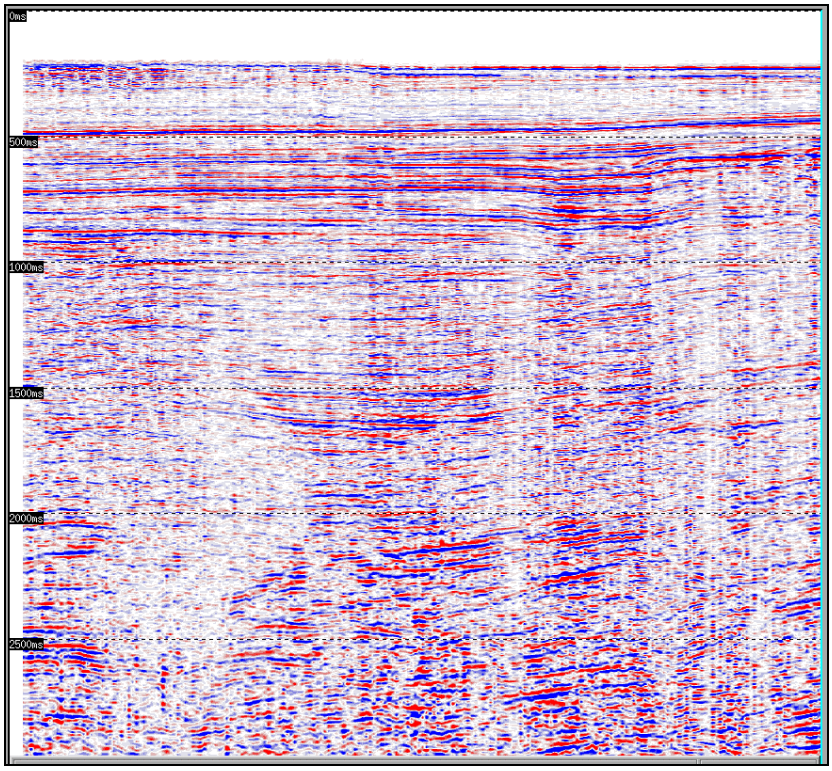


**Figure 22: Single offset over the merge area after regularisation**

### *4.2.8 Residual Demultiple*

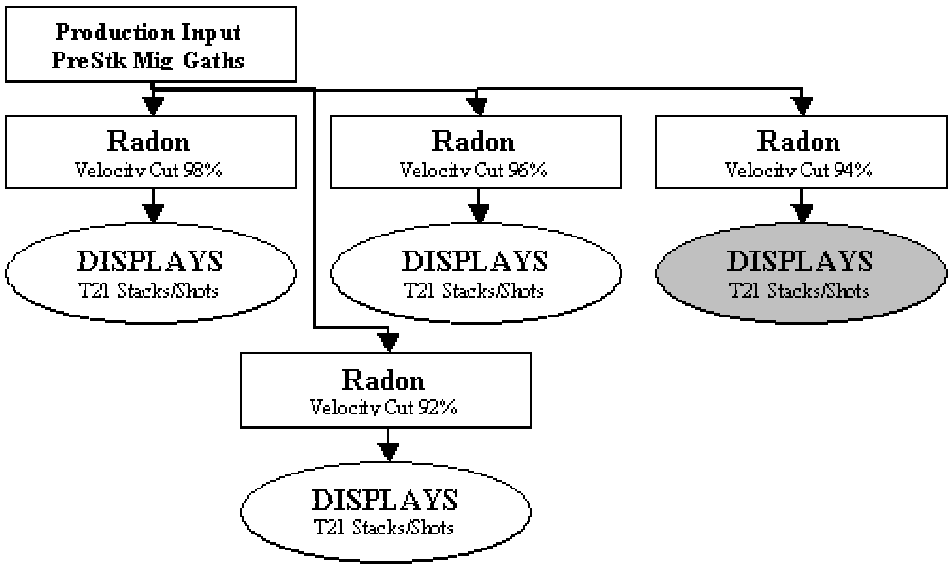

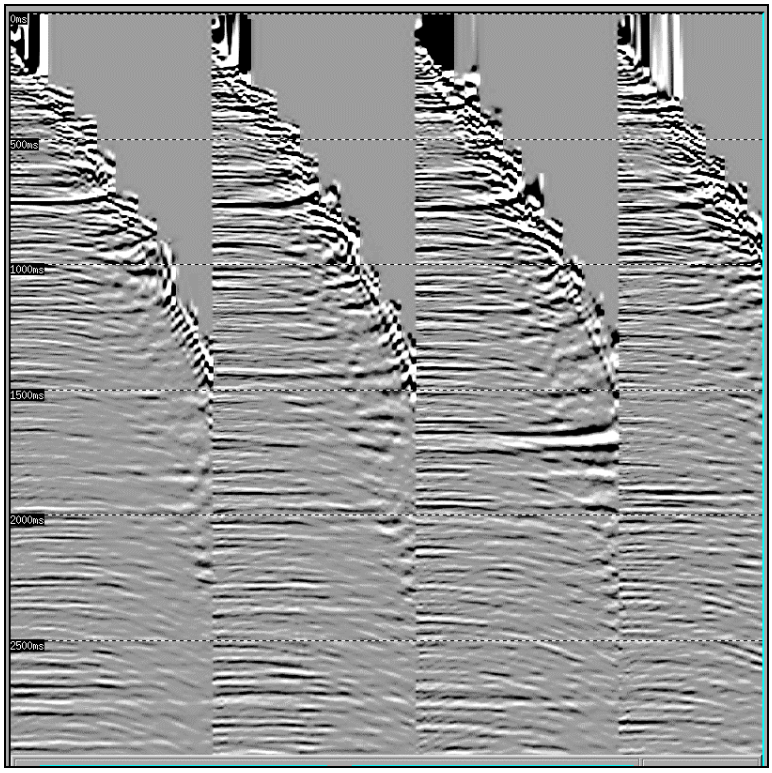


**Figure 23: Selected cmp gathers before residual demultiple**

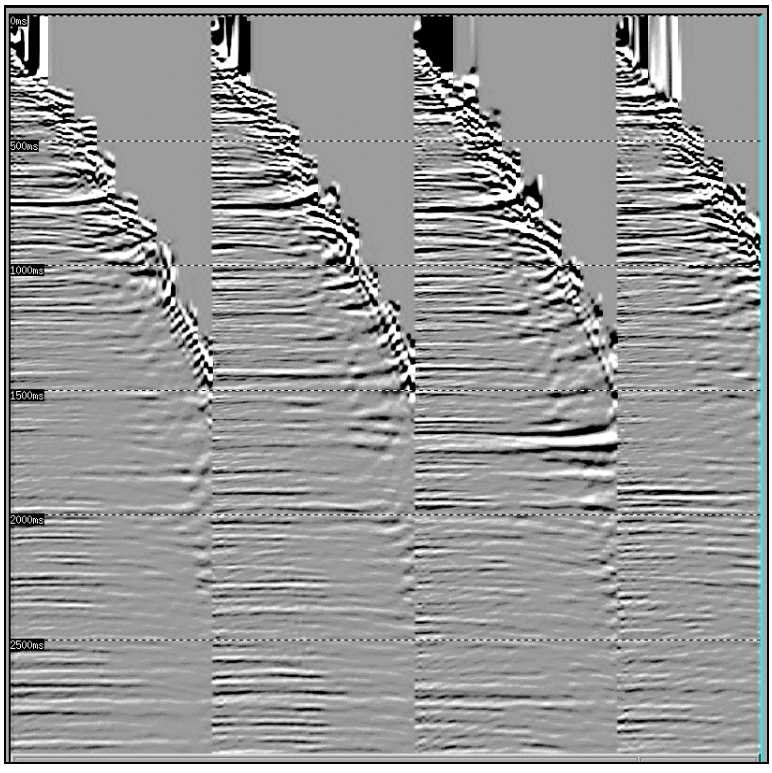


**Figure 24: Selected CMPs gathers after the residual demultiple**

### *4.2.9 CIP RMO*

For the cip_rmo_fit the data had to be run in blocks. Due to the change in fold over the merged dataset, there was a bust, This was because for the block over the merge area all gathers where padded out to 54 fold(cip_rmo_fit only works on full fold gathers, the next block was only 40 fold so there was no way to keep the cip_rmo_fit consistent over the overlap area. There is also a bust in the stack due to change in fold, more evident in the far angle stack as the extra fold is due to far offset

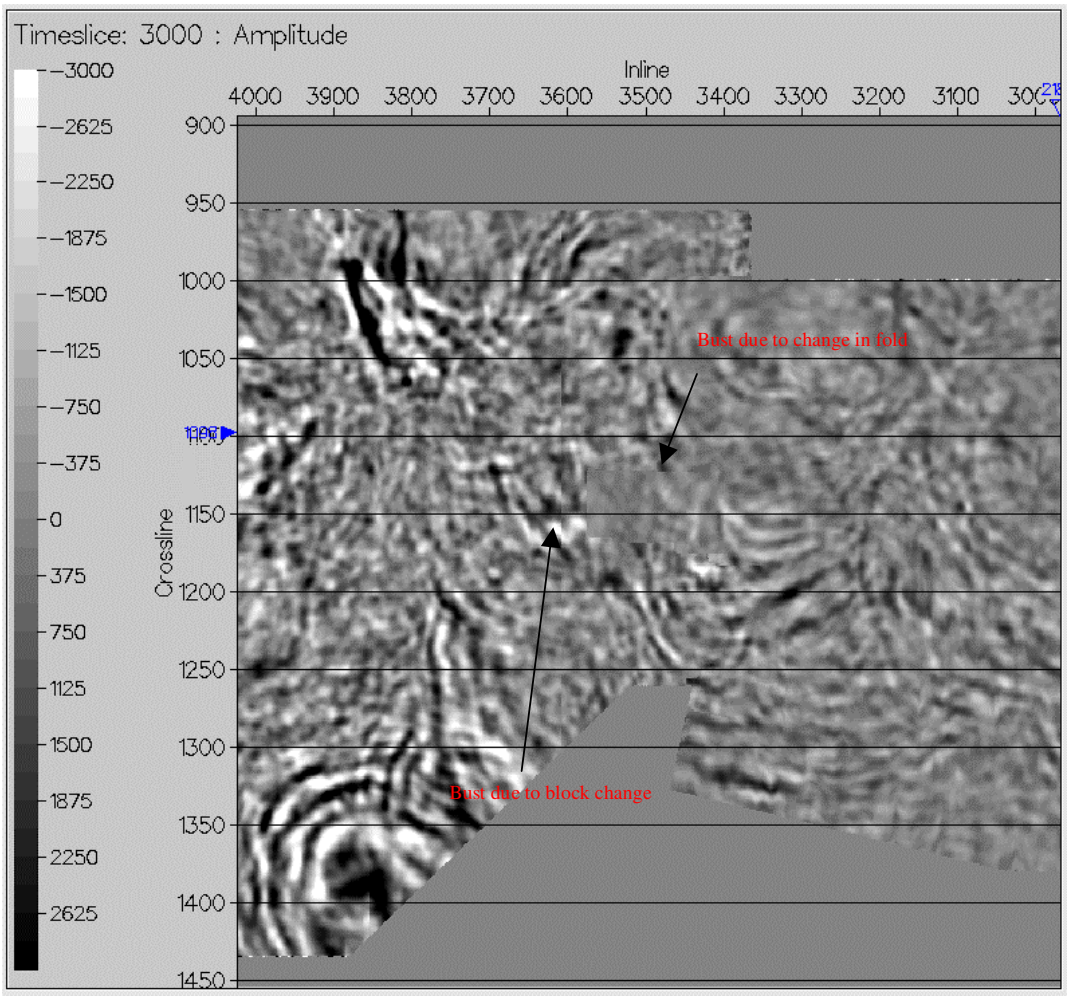


**Figure 25: Bust in seismic due to CIP_RMO**

## *4.3 Signatures/Wavelets*

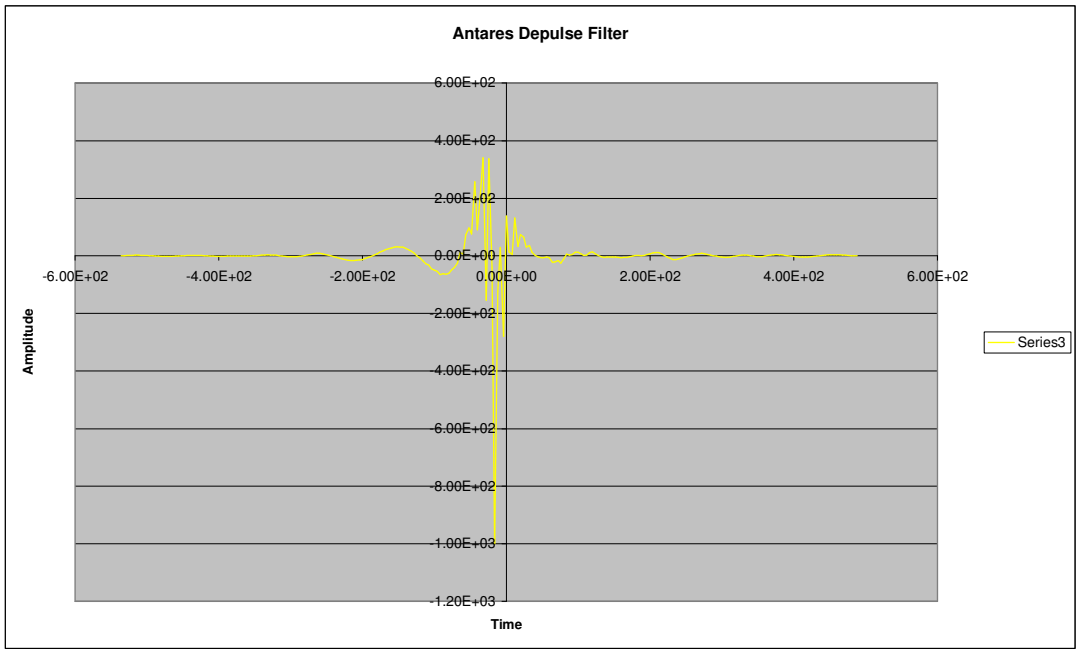


**Figure 26: Antares Depulse Filter**

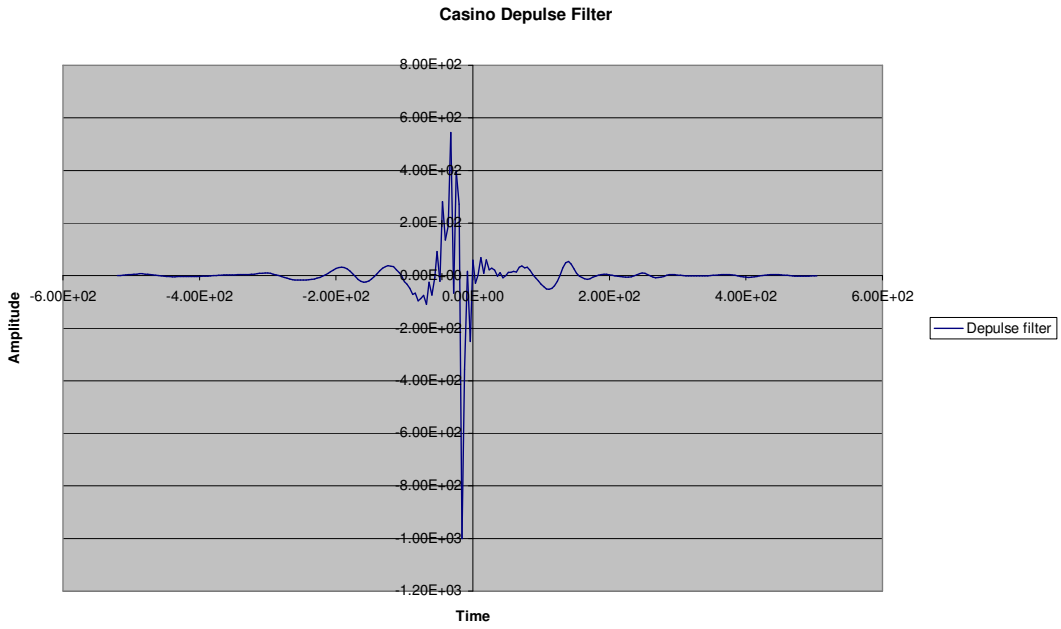


**Figure 27: Casino Depulse Filter**

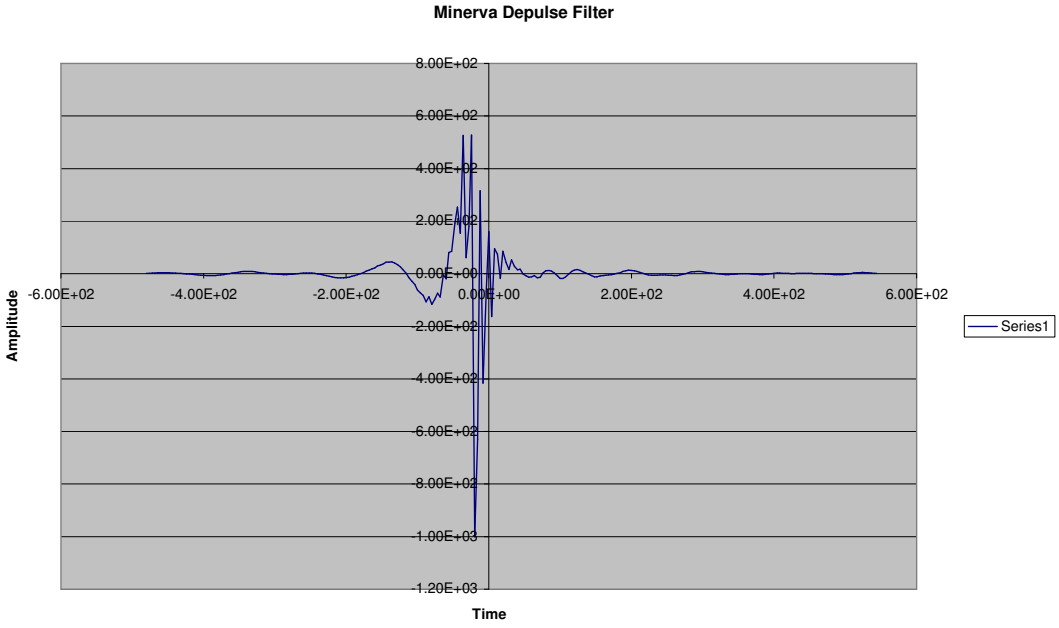


**Figure 28: Minerva Depulse Filter**

## *4.4 Tape Disposition*

### *4.4.1 Full Offset Stacks (SEGY Tape)*

| Tape No | Data Set Name | Inline Range | Date Sent | SL/IL Rel | Remark. |
|---|---|---|---|---|---|
| GW0968 | G1324PST40RMIG.2 | 595-4520 | 28/06/04 | SL=XL | Raw Migration |
| GW0969 | G1324PST40FMIG.2 | 595-4520 | 28/06/07 | SL=XL | Final Migration |
| GW0955 | G1324PST45RMIG.1 | 595-4520 | 02/07/04 | SL=XL | Raw Migration/RMO Gths |

### *4.4.2 Angle Stacks (SEGY Tape)*

| Tape No | Data Set Name | Inline Range | Date Sent | SL/IL Rel | Remark. |
|---|---|---|---|---|---|
| GW0959 | G1324PST40RNFR.1 | 552-4520 | 30/06/04 | SL=XL | Near Angle Stack |
| GW0960 | G1324PST40RNAR.1 | 552-4520 | 30/06/04 | SL=XL | Far Angle Stack |
| GW0961 | G1324PST40RMID.1 | 552-4520 | 30/06/04 | SL=XL | Mid Angle Stack |
| GW0956 | G1324PST45RNFR.1 | 552-4520 | 02/07/04 | SL=XL | Near Angle Stack using CIP |
| GW0957 | G1324PST45RNAR.1 | 552-4520 | 02/07/04 | SL=XL | Far Angle Stack using CIP |
| GW0958 | G1324PST45RMID.1 | 552-4520 | 02/07/04 | SL=XL | Mid Angle Stack using CIP |
| GW0964 | G1324PST45FNFR.1 | 552-4520 | 02/07/04 | SL=XL | Near Angle Stack using CIP |
| GW0967 | G1324PST45FNAR.1 | 552-4520 | 15/07/04 | SL=XL | Far Angle Stack using CIP |
| GW0966 | G1324PST45FMID.1 | 552-4520 | 02/07/04 | SL=XL | Mid Angle Stack using CIP |

### *4.4.3 AVO attribute Stacks (SEGY Tape)*

| Tape No | Data Set Name | Inline Range | Date Sent | SL/IL Rel | Remark. |
|---|---|---|---|---|---|

| | | | | | |
|---|---|---|---|---|---|
| GW0962 | G1324PST45RINT.1 | 552-4520 | 13/07/04 | SL=XL | Intercept Stack using CIP gths |
| GW0963 | G1324PST45RGRA.1 | 552-4520 | 13/07/04 | SL=XL | Gradient Stack using CIP gths |

### *4.4.4 Prestack Migration Gathers (SEGY Tape)*

| Geodetic Parameters | | | |
|---|---|---|---|
| | | | |
| Spheroid : | GDA94, GRS80 | Semi Major Axis : | 6378137 |
| | | Inverse flat : | 298.25 |
| | | | |
| Projection : | UTM, Zone 54s | Grid Origin : | 0000000.000N1410000.00E |
| | | Grid Coord at origin | 50000000.00E10000000.00N |
| | | Scale Factor | 0.9996 |

| Tape No | Data Set Name | Inline Range | | | | Date Sent | SL/IL Rel | Remark. |
|---|---|---|---|---|---|---|---|---|
| | | FST INLINE | LST INLINE | FST XLINE | LST XLINE | | | |
| GW0800 | G1324PST00 | 513 | 828 | 955 | 1435 | 15/07/2004 | SL=XL | Prestack Migration Gths |
| GW0801 | G1324PST00 | 513 | 828 | 955 | 1435 | 15/07/2004 | SL=XL | Prestack Migration Gths |
| GW0802 | G1324PST00 | 513 | 828 | 955 | 1435 | 15/07/2004 | SL=XL | Prestack Migration Gths |
| GW0803 | G1324PST00 | 829 | 1200 | 955 | 1435 | 15/07/2004 | SL=XL | Prestack Migration Gths |
| GW0804 | G1324PST00 | 829 | 1200 | 955 | 1435 | 15/07/2004 | SL=XL | Prestack Migration Gths |
| GW0805 | G1324PST00 | 829 | 1200 | 955 | 1435 | 15/07/2004 | SL=XL | Prestack Migration Gths |
| GW0806 | G1324PST00 | 829 | 1200 | 955 | 1435 | 15/07/2004 | SL=XL | Prestack Migration Gths |
| GW0807 | G1324PST00 | 1201 | 1538 | 955 | 1435 | 15/07/2004 | SL=XL | Prestack Migration Gths |
| GW0808 | G1324PST00 | 1201 | 1538 | 955 | 1435 | 15/07/2004 | SL=XL | Prestack Migration Gths |
| GW0809 | G1324PST00 | 1201 | 1538 | 955 | 1435 | 15/07/2004 | SL=XL | Prestack Migration Gths |
| GW0810 | G1324PST00 | 1201 | 1538 | 955 | 1435 | 15/07/2004 | SL=XL | Prestack Migration Gths |
| GW0811 | G1324PST00 | 1539 | 1820 | 955 | 1435 | 15/07/2004 | SL=XL | Prestack Migration Gths |
| GW0812 | G1324PST00 | 1539 | 1820 | 955 | 1435 | 15/07/2004 | SL=XL | Prestack Migration Gths |
| GW0813 | G1324PST00 | 1539 | 1820 | 955 | 1435 | 15/07/2004 | SL=XL | Prestack Migration Gths |
| GW0814 | G1324PST00 | 1821 | 2070 | 955 | 1435 | 15/07/2004 | SL=XL | Prestack Migration Gths |
| GW0815 | G1324PST00 | 1821 | 2070 | 955 | 1435 | 15/07/2004 | SL=XL | Prestack Migration Gths |
| GW0816 | G1324PST00 | 1821 | 2070 | 955 | 1435 | 15/07/2004 | SL=XL | Prestack Migration Gths |
| GW0817 | G1324PST00 | 2071 | 2311 | 955 | 1435 | 15/07/2004 | SL=XL | Prestack Migration Gths |
| GW0818 | G1324PST00 | 2071 | 2311 | 955 | 1435 | 15/07/2004 | SL=XL | Prestack Migration Gths |
| GW0819 | G1324PST00 | 2071 | 2311 | 955 | 1435 | 15/07/2004 | SL=XL | Prestack Migration Gths |
| GW0820 | G1324PST00 | 2312 | 2555 | 955 | 1435 | 15/07/2004 | SL=XL | Prestack Migration Gths |
| GW0821 | G1324PST00 | 2312 | 2555 | 955 | 1435 | 15/07/2004 | SL=XL | Prestack Migration Gths |
| GW0822 | G1324PST00 | 2312 | 2555 | 955 | 1435 | 15/07/2004 | SL=XL | Prestack Migration Gths |
| GW0823 | G1324PST00 | 2312 | 2555 | 955 | 1435 | 15/07/2004 | SL=XL | Prestack Migration Gths |
| GW0824 | G1324PST00 | 2556 | 2803 | 955 | 1435 | 15/07/2004 | SL=XL | Prestack Migration Gths |
| GW0825 | G1324PST00 | 2556 | 2803 | 955 | 1435 | 15/07/2004 | SL=XL | Prestack Migration Gths |
| GW0826 | G1324PST00 | 2556 | 2803 | 955 | 1435 | 15/07/2004 | SL=XL | Prestack Migration Gths |
| GW0827 | G1324PST00 | 2556 | 2803 | 955 | 1435 | 15/07/2004 | SL=XL | Prestack Migration Gths |
| GW0828 | G1324PST00 | 2804 | 3058 | 955 | 1435 | 15/07/2004 | SL=XL | Prestack Migration Gths |
| GW0829 | G1324PST00 | 2804 | 3058 | 955 | 1435 | 15/07/2004 | SL=XL | Prestack Migration Gths |
| GW0830 | G1324PST00 | 2804 | 3058 | 955 | 1435 | 15/07/2004 | SL=XL | Prestack Migration Gths |
| GW0831 | G1324PST00 | 2804 | 3058 | 955 | 1435 | 15/07/2004 | SL=XL | Prestack Migration Gths |
| GW0832 | G1324PST00 | 3059 | 3328 | 955 | 1435 | 15/07/2004 | SL=XL | Prestack Migration Gths |
| GW0833 | G1324PST00 | 3059 | 3328 | 955 | 1435 | 15/07/2004 | SL=XL | Prestack Migration Gths |
| GW0834 | G1324PST00 | 3059 | 3328 | 955 | 1435 | 15/07/2004 | SL=XL | Prestack Migration Gths |

| | | | | | | | | |
|---|---|---|---|---|---|---|---|---|
| GW0835 | G1324PST00 | 3059 | 3328 | 955 | 1435 | 15/07/2004 | SL=XL | Prestack Migration Gths |
| GW0836 | G1324PST00 | 3329 | 3607 | 955 | 1435 | 15/07/2004 | SL=XL | Prestack Migration Gths |
| GW0837 | G1324PST00 | 3329 | 3607 | 955 | 1435 | 15/07/2004 | SL=XL | Prestack Migration Gths |
| GW0838 | G1324PST00 | 3329 | 3607 | 955 | 1435 | 15/07/2004 | SL=XL | Prestack Migration Gths |
| GW0839 | G1324PST00 | 3608 | 3853 | 955 | 1435 | 15/07/2004 | SL=XL | Prestack Migration Gths |
| GW0840 | G1324PST00 | 3608 | 3853 | 955 | 1435 | 15/07/2004 | SL=XL | Prestack Migration Gths |
| GW0841 | G1324PST00 | 3608 | 3853 | 955 | 1435 | 15/07/2004 | SL=XL | Prestack Migration Gths |
| GW0842 | G1324PST00 | 3854 | 4063 | 955 | 1435 | 15/07/2004 | SL=XL | Prestack Migration Gths |
| GW0843 | G1324PST00 | 3854 | 4063 | 955 | 1435 | 15/07/2004 | SL=XL | Prestack Migration Gths |
| GW0844 | G1324PST00 | 3854 | 4063 | 955 | 1435 | 15/07/2004 | SL=XL | Prestack Migration Gths |
| GW0845 | G1324PST00 | 4064 | 4270 | 955 | 1435 | 15/07/2004 | SL=XL | Prestack Migration Gths |
| GW0846 | G1324PST00 | 4064 | 4270 | 955 | 1435 | 15/07/2004 | SL=XL | Prestack Migration Gths |
| GW0847 | G1324PST00 | 4064 | 4270 | 955 | 1435 | 15/07/2004 | SL=XL | Prestack Migration Gths |
| GW0848 | G1324PST00 | 4271 | 4600 | 955 | 1435 | 15/07/2004 | SL=XL | Prestack Migration Gths |
| GW0849 | G1324PST00 | 4271 | 4600 | 955 | 1435 | 15/07/2004 | SL=XL | Prestack Migration Gths |
| GW0850 | G1324PST00 | 4271 | 4600 | 955 | 1435 | 15/07/2004 | SL=XL | Prestack Migration Gths |
| GW0851 | G1324PST00 | 4271 | 4600 | 955 | 1435 | 15/07/2004 | SL=XL | Prestack Migration Gths |

### *4.4.5 Navigation Merged Gathers (Antares)*

| Geodetic Parameters | | | |
|---|---|---|---|
| | | | |
| Spheroid : | GDA94, GRS80 | Semi Major Axis : | 6378137 |
| | | Inverse flat : | 298.25 |
| | | | |
| Projection : | UTM, Zone 54s | Grid Origin : | 0000000.000N1410000.00E |
| | | Grid Coord at origin | 50000000.00E10000000.00N |
| | | Scale Factor | 0.9996 |

| Tape No | LINE | FIRST SP | LAST SP | Date Sent | SL/IL Rel | Remark. |
|---|---|---|---|---|---|---|
| GW0710 | WO3ANT1116P2 | 1782 | 2944 | 1/9/2004 | SL=IL | After Swatt/Fk |
| GW0711 | WO3ANT1156P1 | 2836 | 893 | 1/9/2004 | SL=IL | After Swatt/Fk |
| GW0712 | WO3ANT1156P1 | 2836 | 893 | 1/9/2004 | SL=IL | After Swatt/Fk |
| GW0713 | WO3ANT1108P1 | 1001 | 2944 | 1/9/2004 | SL=IL | After Swatt/Fk |
| GW0714 | WO3ANT1108P1 | 1001 | 2944 | 1/9/2004 | SL=IL | After Swatt/Fk |
| GW0715 | WO3ANT1148P1 | 2836 | 893 | 1/9/2004 | SL=IL | After Swatt/Fk |
| GW0716 | WO3ANT1148P1 | 2836 | 893 | 1/9/2004 | SL=IL | After Swatt/Fk |
| GW0717 | WO3ANT1036P1 | 1001 | 2944 | 1/9/2004 | SL=IL | After Swatt/Fk |
| GW0718 | WO3ANT1036P1 | 1001 | 2944 | 1/9/2004 | SL=IL | After Swatt/Fk |
| GW0719 | WO3ANT1140P1 | 2836 | 893 | 1/9/2004 | SL=IL | After Swatt/Fk |
| GW0720 | WO3ANT1140P1 | 2836 | 893 | 1/9/2004 | SL=IL | After Swatt/Fk |
| GW0721 | WO3ANT1100P1 | 1001 | 2944 | 1/9/2004 | SL=IL | After Swatt/Fk |
| GW0722 | WO3ANT1100P1 | 1001 | 2944 | 1/9/2004 | SL=IL | After Swatt/Fk |
| GW0723 | WO3ANT1132P1 | 2836 | 893 | 1/9/2004 | SL=IL | After Swatt/Fk |
| GW0724 | WO3ANT1132P1 | 2836 | 893 | 1/9/2004 | SL=IL | After Swatt/Fk |
| GW0725 | WO3ANT1004P1 | 1022 | 2944 | 1/9/2004 | SL=IL | After Swatt/Fk |
| GW0726 | WO3ANT1004P1 | 1022 | 2944 | 1/9/2004 | SL=IL | After Swatt/Fk |
| GW0727 | WO3ANT1124P1 | 2836 | 1678 | 1/9/2004 | SL=IL | After Swatt/Fk |
| GW0728 | WO3ANT1124P2 | 1687 | 893 | 1/9/2004 | SL=IL | After Swatt/Fk |
| GW0729 | WO3ANT1012P1 | 1001 | 2944 | 1/9/2004 | SL=IL | After Swatt/Fk |

| | | | | | | |
|---|---|---|---|---|---|---|
| GW0730 | WO3ANT1012P1 | 1001 | 2944 | 1/9/2004 | SL=IL | After Swatt/Fk |
| GW0731 | WO3ANT1092P1 | 1100 | 2944 | 1/9/2004 | SL=IL | After Swatt/Fk |
| GW0732 | WO3ANT1092P1 | 1100 | 2944 | 1/9/2004 | SL=IL | After Swatt/Fk |
| GW0733 | WO3ANT1164P1 | 2813 | 893 | 1/9/2004 | SL=IL | After Swatt/Fk |
| GW0734 | WO3ANT1164P1 | 2813 | 893 | 1/9/2004 | SL=IL | After Swatt/Fk |
| GW0735 | WO3ANT1012P1 | 2092 | 2153 | 1/9/2004 | SL=IL | After Swatt/Fk |
| GW0736 | WO3ANT1260P1 | 2168 | 893 | 1/9/2004 | SL=IL | After Swatt/Fk |
| GW0737 | WO3ANT1260P1 | 2168 | 893 | 1/9/2004 | SL=IL | After Swatt/Fk |
| GW0738 | WO3ANT1044P1 | 1001 | 2944 | 1/9/2004 | SL=IL | After Swatt/Fk |
| GW0739 | WO3ANT1044P1 | 1001 | 2944 | 1/9/2004 | SL=IL | After Swatt/Fk |
| GW0740 | WO3ANT1172P1 | 2759 | 893 | 1/9/2004 | SL=IL | After Swatt/Fk |
| GW0741 | WO3ANT1172P1 | 2759 | 893 | 1/9/2004 | SL=IL | After Swatt/Fk |
| GW0742 | WO3ANT1020P1 | 1001 | 2944 | 1/9/2004 | SL=IL | After Swatt/Fk |
| GW0743 | WO3ANT1020P1 | 1001 | 2944 | 1/9/2004 | SL=IL | After Swatt/Fk |
| GW0744 | WO3ANT1180P1 | 2730 | 893 | 1/9/2004 | SL=IL | After Swatt/Fk |
| GW0745 | WO3ANT1180P1 | 2730 | 893 | 1/9/2004 | SL=IL | After Swatt/Fk |
| GW0746 | WO3ANT1052P1 | 1001 | 2944 | 1/9/2004 | SL=IL | After Swatt/Fk |
| GW0747 | WO3ANT1052P1 | 1001 | 2944 | 1/9/2004 | SL=IL | After Swatt/Fk |
| GW0748 | WO3ANT1188P1 | 2658 | 893 | 1/9/2004 | SL=IL | After Swatt/Fk |
| GW0749 | WO3ANT1188P1 | 2658 | 893 | 1/9/2004 | SL=IL | After Swatt/Fk |
| GW0750 | WO3ANT1028P1 | 1001 | 2944 | 1/9/2004 | SL=IL | After Swatt/Fk |
| GW0751 | WO3ANT1028P1 | 1001 | 2944 | 1/9/2004 | SL=IL | After Swatt/Fk |
| GW0752 | WO3ANT1196P1 | 2634 | 893 | 1/9/2004 | SL=IL | After Swatt/Fk |
| GW0753 | WO3ANT1196P1 | 2634 | 893 | 1/9/2004 | SL=IL | After Swatt/Fk |
| GW0754 | WO3ANT1020I1 | 1001 | 2944 | 1/9/2004 | SL=IL | After Swatt/Fk |
| GW0755 | WO3ANT1020I1 | 1001 | 2944 | 1/9/2004 | SL=IL | After Swatt/Fk |
| GW0756 | WO3ANT1196I2 | 2598 | 893 | 1/9/2004 | SL=IL | After Swatt/Fk |
| GW0757 | WO3ANT1196I2 | 2598 | 893 | 1/9/2004 | SL=IL | After Swatt/Fk |
| GW0758 | WO3ANT1060P1 | 1231 | 2944 | 1/9/2004 | SL=IL | After Swatt/Fk |
| GW0759 | WO3ANT1060P1 | 1231 | 2944 | 1/9/2004 | SL=IL | After Swatt/Fk |
| GW0760 | WO3ANT1204P1 | 2544 | 893 | 1/9/2004 | SL=IL | After Swatt/Fk |
| GW0761 | WO3ANT1204P1 | 2544 | 893 | 1/9/2004 | SL=IL | After Swatt/Fk |
| GW0762 | WO3ANT1068P1 | 1001 | 2944 | 1/9/2004 | SL=IL | After Swatt/Fk |
| GW0763 | WO3ANT1068P1 | 1001 | 2944 | 1/9/2004 | SL=IL | After Swatt/Fk |
| GW0764 | WO3ANT1212P1 | 2525 | 893 | 1/9/2004 | SL=IL | After Swatt/Fk |
| GW0765 | WO3ANT1212P1 | 2525 | 893 | 1/9/2004 | SL=IL | After Swatt/Fk |
| GW0766 | WO3ANT1076P1 | 1003 | 2944 | 1/9/2004 | SL=IL | After Swatt/Fk |
| GW0767 | WO3ANT1076P1 | 1003 | 2944 | 1/9/2004 | SL=IL | After Swatt/Fk |
| GW0768 | WO3ANT1220P1 | 2478 | 893 | 1/9/2004 | SL=IL | After Swatt/Fk |
| GW0769 | WO3ANT1220P1 | 2478 | 893 | 1/9/2004 | SL=IL | After Swatt/Fk |
| GW0770 | WO3ANT1084P1 | 1001 | 2944 | 1/9/2004 | SL=IL | After Swatt/Fk |
| GW0771 | WO3ANT1084P1 | 1001 | 2944 | 1/9/2004 | SL=IL | After Swatt/Fk |
| GW0772 | WO3ANT1228P1 | 2423 | 893 | 1/9/2004 | SL=IL | After Swatt/Fk |
| GW0773 | WO3ANT1228P1 | 2423 | 893 | 1/9/2004 | SL=IL | After Swatt/Fk |
| GW0774 | WO3ANT1084I1 | 1001 | 2944 | 1/9/2004 | SL=IL | After Swatt/Fk |
| GW0775 | WO3ANT1084I1 | 1001 | 2944 | 1/9/2004 | SL=IL | After Swatt/Fk |
| GW0776 | WO3ANT1236P1 | 2372 | 893 | 1/9/2004 | SL=IL | After Swatt/Fk |
| GW0777 | WO3ANT1236P1 | 2372 | 893 | 1/9/2004 | SL=IL | After Swatt/Fk |
| GW0778 | WO3ANT1116I1 | 1001 | 2944 | 1/9/2004 | SL=IL | After Swatt/Fk |

| | | | | | | |
|---|---|---|---|---|---|---|
| GW0779 | WO3ANT1116I1 | 1001 | 2944 | 1/9/2004 | SL=IL | After Swatt/Fk |
| GW0780 | WO3ANT1180P2 | 2588 | 2415 | 1/9/2004 | SL=IL | After Swatt/Fk |
| GW0781 | WO3ANT1196P2 | 2106 | 1949 | 1/9/2004 | SL=IL | After Swatt/Fk |
| GW0782 | WO3ANT1244P1 | 2319 | 893 | 1/9/2004 | SL=IL | After Swatt/Fk |
| GW0783 | WO3ANT1244P1 | 2319 | 893 | 1/9/2004 | SL=IL | After Swatt/Fk |
| GW0784 | WO3ANT1116P3 | 1001 | 1791 | 1/9/2004 | SL=IL | After Swatt/Fk |
| GW0785 | WO3ANT1212P2 | 1938 | 1763 | 1/9/2004 | SL=IL | After Swatt/Fk |
| GW0786 | WO3ANT1252P1 | 2265 | 893 | 1/9/2004 | SL=IL | After Swatt/Fk |
| GW0787 | WO3ANT1252P1 | 2265 | 893 | 1/9/2004 | SL=IL | After Swatt/Fk |
| GW0788 | WO3ANT1092P2 | 1001 | 1109 | 1/9/2004 | SL=IL | After Swatt/Fk |
| GW0789 | WO3ANT1092P3 | 2102 | 2220 | 1/9/2004 | SL=IL | After Swatt/Fk |
| GW0790 | WO3ANT1252I1 | 2222 | 893 | 1/9/2004 | SL=IL | After Swatt/Fk |
| GW0791 | WO3ANT1252I1 | 2222 | 893 | 1/9/2004 | SL=IL | After Swatt/Fk |
| GW0792 | WO3ANT1060P2 | 1001 | 1240 | 1/9/2004 | SL=IL | After Swatt/Fk |
| GW0793 | WO3ANT1116P2 | 1782 | 2944 | 1/9/2004 | SL=IL | After Swatt/Fk |
| GW0794 | WO3ANT1124P1 | 2836 | 1678 | 1/9/2004 | SL=IL | After Swatt/Fk |

### *4.4.6 Navigation Merged Gathers (Casino)*

| Geodetic Parameters | | | |
|---|---|---|---|
| | | | |
| Spheroid : | GDA94, GRS80 | Semi Major Axis : | 6378137 |
| | | Inverse flat : | 298.25 |
| | | | |
| Projection : | UTM, Zone 54s | Grid Origin : | 0000000.000N1410000.00E |
| | | Grid Coord at origin | 50000000.00E10000000.00N |
| | | Scale Factor | 0.9996 |

| Tape No | LINE | FIRST SP | LAST SP | Date Sent | SL/IL Rel | Remark. |
|---|---|---|---|---|---|---|
| GW0852 | S01CAS2249P056 | 2511 | 1177 | 1/09/2004 | SL=IL | After Swatt/Fk |
| GW0853 | S01CAS2249P056 | 2511 | 1177 | 1/09/2004 | SL=IL | After Swatt/Fk |
| GW0854 | S01CAS2105P057 | 1283 | 2039 | 1/09/2004 | SL=IL | After Swatt/Fk |
| GW0856 | S01CAS2237P058 | 2511 | 1177 | 1/09/2004 | SL=IL | After Swatt/Fk |
| GW0857 | S01CAS2237P058 | 2511 | 1177 | 1/09/2004 | SL=IL | After Swatt/Fk |
| GW0858 | S01CAS2093P059 | 1283 | 2619 | 1/09/2004 | SL=IL | After Swatt/Fk |
| GW0859 | S01CAS2225P060 | 2512 | 1177 | 1/09/2004 | SL=IL | After Swatt/Fk |
| GW0860 | S01CAS2225P060 | 2512 | 1177 | 1/09/2004 | SL=IL | After Swatt/Fk |
| GW0861 | S01CAS2081P061 | 1283 | 2619 | 1/09/2004 | SL=IL | After Swatt/Fk |
| GW0862 | S01CAS2213P062 | 2512 | 1177 | 1/09/2004 | SL=IL | After Swatt/Fk |
| GW0863 | S01CAS2213P062 | 2512 | 1177 | 1/09/2004 | SL=IL | After Swatt/Fk |
| GW0864 | S01CAS2069P065 | 1283 | 2670 | 1/09/2004 | SL=IL | After Swatt/Fk |
| GW0865 | S01CAS2201P066 | 2512 | 1177 | 1/09/2004 | SL=IL | After Swatt/Fk |
| GW0866 | S01CAS2201P066 | 2512 | 1177 | 1/09/2004 | SL=IL | After Swatt/Fk |
| GW0867 | S01CAS2057P067 | 1283 | 2670 | 1/09/2004 | SL=IL | After Swatt/Fk |
| GW0868 | S01CAS2189P068 | 2512 | 1177 | 1/09/2004 | SL=IL | After Swatt/Fk |
| GW0869 | S01CAS2189P068 | 2512 | 1177 | 1/09/2004 | SL=IL | After Swatt/Fk |
| GW0870 | S01CAS2177P071 | 2512 | 1177 | 1/09/2004 | SL=IL | After Swatt/Fk |
| GW0871 | S01CAS2177P071 | 2512 | 1177 | 1/09/2004 | SL=IL | After Swatt/Fk |
| GW0872 | S01CAS2165P073 | 2512 | 1177 | 1/09/2004 | SL=IL | After Swatt/Fk |
| GW0873 | S01CAS2165P073 | 2512 | 1177 | 1/09/2004 | SL=IL | After Swatt/Fk |
| GW0874 | S01CAS2153P075 | 2512 | 1177 | 1/09/2004 | SL=IL | After Swatt/Fk |
| GW0875 | S01CAS2153P075 | 2512 | 1177 | 1/09/2004 | SL=IL | After Swatt/Fk |

| | | | | | | |
|---|---|---|---|---|---|---|
| GW0876 | S01CAS2141P077 | 2513 | 1177 | 1/09/2004 | SL=IL | After Swatt/Fk |
| GW0877 | S01CAS2141P077 | 2513 | 1177 | 1/09/2004 | SL=IL | After Swatt/Fk |
| GW0878 | S01CAS2129P079 | 2513 | 1177 | 1/09/2004 | SL=IL | After Swatt/Fk |
| GW0879 | S01CAS2129P079 | 2513 | 1177 | 1/09/2004 | SL=IL | After Swatt/Fk |
| GW0880 | S01CAS2117P081 | 2513 | 1177 | 1/09/2004 | SL=IL | After Swatt/Fk |
| GW0881 | S01CAS2117P081 | 2513 | 1177 | 1/09/2004 | SL=IL | After Swatt/Fk |
| GW0882 | S01CAS2117J083 | 2513 | 1177 | 1/09/2004 | SL=IL | After Swatt/Fk |
| GW0883 | S01CAS2117J083 | 2513 | 1177 | 1/09/2004 | SL=IL | After Swatt/Fk |

### *4.4.7 Navigation Merged Gathers (Minerva)*

| Geodetic Parameters | | | |
|---|---|---|---|
| | | | |
| Spheroid : | AGD84,ANS | Semi Major Axis : | 6378160 |
| | | Inverse flat : | 298.25 |
| | | | |
| Projection : | UTM, Zone 54s | Grid Origin : | 0000000.000N1410000.00E |
| | | Grid Coord at origin | 50000000.00E10000000.00N |
| | | Scale Factor | 0.9996 |

| Tape No | LINE | FIRST SP | LAST SP | Date Sent | SL/IL Rel | Remark. |
|---|---|---|---|---|---|---|
| GW0884 | OH94-1344 | 1117 | 1769 | 1/09/2004 | SL=IL | After Swatt/FK |
| GW0885 | OH94-1104 | 1669 | 906 | 1/09/2004 | SL=IL | After Swatt/FK |
| GW0886 | OH94-1336 | 1107 | 1764 | 1/09/2004 | SL=IL | After Swatt/FK |
| GW0887 | OH94-1096 | 1655 | 906 | 1/09/2004 | SL=IL | After Swatt/FK |
| GW0888 | OH94-1328 | 1110 | 1764 | 1/09/2004 | SL=IL | After Swatt/FK |
| GW0889 | OH94-1000 | 1655 | 906 | 1/09/2004 | SL=IL | After Swatt/FK |
| GW0890 | OH94-1320 | 1099 | 1764 | 1/09/2004 | SL=IL | After Swatt/FK |
| GW0891 | OH94-1088 | 1655 | 906 | 1/09/2004 | SL=IL | After Swatt/FK |
| GW0892 | OH94-1312 | 1088 | 1764 | 1/09/2004 | SL=IL | After Swatt/FK |
| GW0893 | OH94-1008A | 1655 | 906 | 1/09/2004 | SL=IL | After Swatt/FK |
| GW0894 | OH94-1304 | 1078 | 1764 | 1/09/2004 | SL=IL | After Swatt/FK |
| GW0895 | OH94-1016 | 1655 | 906 | 1/09/2004 | SL=IL | After Swatt/FK |
| GW0896 | OH94-1024 | 1655 | 906 | 1/09/2004 | SL=IL | After Swatt/FK |
| GW0897 | OH94-1296 | 1067 | 1764 | 1/09/2004 | SL=IL | After Swatt/FK |
| GW0898 | OH94-1112 | 1655 | 906 | 1/09/2004 | SL=IL | After Swatt/FK |
| GW0899 | OH94-1120 | 1655 | 906 | 1/09/2004 | SL=IL | After Swatt/FK |
| GW0900 | OH94-1352 | 1142 | 1764 | 1/09/2004 | SL=IL | After Swatt/FK |
| GW0901 | OH94-1040 | 1655 | 906 | 1/09/2004 | SL=IL | After Swatt/FK |
| GW0902 | OH94-1280 | 1046 | 1764 | 1/09/2004 | SL=IL | After Swatt/FK |
| GW0903 | OH94-1080 | 1655 | 906 | 1/09/2004 | SL=IL | After Swatt/FK |
| GW0904 | OH94-1272 | 1035 | 1764 | 1/09/2004 | SL=IL | After Swatt/FK |
| GW0905 | OH94-1072 | 1655 | 906 | 1/09/2004 | SL=IL | After Swatt/FK |
| GW0906 | OH94-1264 | 1024 | 1764 | 1/09/2004 | SL=IL | After Swatt/FK |
| GW0907 | OH94-1048 | 1655 | 906 | 1/09/2004 | SL=IL | After Swatt/FK |
| GW0908 | OH94-1256 | 1015 | 1764 | 1/09/2004 | SL=IL | After Swatt/FK |
| GW0909 | OH94-1128 | 1655 | 906 | 1/09/2004 | SL=IL | After Swatt/FK |
| GW0910 | OH94-1360 | 1153 | 1764 | 1/09/2004 | SL=IL | After Swatt/FK |
| GW0911 | OH94-1192 | 1655 | 906 | 1/09/2004 | SL=IL | After Swatt/FK |
| GW0912 | OH94-1368 | 1163 | 1764 | 1/09/2004 | SL=IL | After Swatt/FK |
| GW0913 | OH94-1056 | 1655 | 906 | 1/09/2004 | SL=IL | After Swatt/FK |
| GW0914 | OH94-1376 | 1174 | 1764 | 1/09/2004 | SL=IL | After Swatt/FK |
| GW0915 | OH94-1136 | 1655 | 906 | 1/09/2004 | SL=IL | After Swatt/FK |
| GW0916 | OH94-1384 | 1185 | 1764 | 1/09/2004 | SL=IL | After Swatt/FK |

| | | | | | | |
|---|---|---|---|---|---|---|
| GW0917 | OH94-1032A | 1655 | 906 | 1/09/2004 | SL=IL | After Swatt/FK |
| GW0918 | OH94-1064 | 1655 | 906 | 1/09/2004 | SL=IL | After Swatt/FK |
| GW0919 | OH94-1392 | 1196 | 1764 | 1/09/2004 | SL=IL | After Swatt/FK |
| GW0920 | OH94-1000I | 1655 | 906 | 1/09/2004 | SL=IL | After Swatt/FK |
| GW0921 | OH94-1248A | 1015 | 1764 | 1/09/2004 | SL=IL | After Swatt/FK |
| GW0922 | OH94-1064I | 1655 | 906 | 1/09/2004 | SL=IL | After Swatt/FK |
| GW0923 | OH94-1280A | 1150 | 1639 | 1/09/2004 | SL=IL | After Swatt/FK |
| GW0924 | OH94-1072I | 1655 | 906 | 1/09/2004 | SL=IL | After Swatt/FK |
| GW0925 | OH94-1400 | 1206 | 1764 | 1/09/2004 | SL=IL | After Swatt/FK |
| GW0926 | OH94-1184 | 1655 | 906 | 1/09/2004 | SL=IL | After Swatt/FK |
| GW0927 | OH94-1408 | 1217 | 1764 | 1/09/2004 | SL=IL | After Swatt/FK |
| GW0928 | OH94-1144 | 1655 | 906 | 1/09/2004 | SL=IL | After Swatt/FK |
| GW0929 | OH94-1416 | 1228 | 1764 | 1/09/2004 | SL=IL | After Swatt/FK |
| GW0930 | OH94-1176 | 1655 | 906 | 1/09/2004 | SL=IL | After Swatt/FK |
| GW0931 | OH94-1424 | 1238 | 1764 | 1/09/2004 | SL=IL | After Swatt/FK |
| GW0932 | OH94-1200 | 1655 | 906 | 1/09/2004 | SL=IL | After Swatt/FK |
| GW0933 | OH94-1432 | 1249 | 1764 | 1/09/2004 | SL=IL | After Swatt/FK |
| GW0934 | OH94-1168 | 1655 | 906 | 1/09/2004 | SL=IL | After Swatt/FK |
| GW0935 | OH94-1440 | 1260 | 1764 | 1/09/2004 | SL=IL | After Swatt/FK |
| GW0936 | OH94-1160 | 1655 | 906 | 1/09/2004 | SL=IL | After Swatt/FK |
| GW0937 | OH94-1448 | 1270 | 1764 | 1/09/2004 | SL=IL | After Swatt/FK |
| GW0938 | OH94-1152 | 1655 | 906 | 1/09/2004 | SL=IL | After Swatt/FK |
| GW0939 | OH94-1456 | 1281 | 1764 | 1/09/2004 | SL=IL | After Swatt/FK |
| GW0940 | OH94-1152I | 1655 | 906 | 1/09/2004 | SL=IL | After Swatt/FK |
| GW0941 | OH94-1288A | 1056 | 1764 | 1/09/2004 | SL=IL | After Swatt/FK |
| GW0942 | OH94-1208 | 1655 | 906 | 1/09/2004 | SL=IL | After Swatt/FK |
| GW0943 | OH94-1456I | 1281 | 1764 | 1/09/2004 | SL=IL | After Swatt/FK |
| GW0944 | OH94-1216 | 1655 | 906 | 1/09/2004 | SL=IL | After Swatt/FK |
| GW0945 | OH94-1464A | 1292 | 1764 | 1/09/2004 | SL=IL | After Swatt/FK |
| GW0946 | OH94-1224 | 1655 | 906 | 1/09/2004 | SL=IL | After Swatt/FK |
| GW0947 | OH94-1472 | 1303 | 1764 | 1/09/2004 | SL=IL | After Swatt/FK |
| GW0948 | OH94-1232 | 1655 | 906 | 1/09/2004 | SL=IL | After Swatt/FK |
| GW0949 | OH94-1480 | 1313 | 1764 | 1/09/2004 | SL=IL | After Swatt/FK |
| GW0950 | OH94-1240 | 1655 | 906 | 1/09/2004 | SL=IL | After Swatt/FK |
| GW0951 | OH94-1248I | 1015 | 1764 | 1/09/2004 | SL=IL | After Swatt/FK |
| GW0952 | OH94-1240I | 1655 | 906 | 1/09/2004 | SL=IL | After Swatt/FK |
| GW0953 | OH94-1328I | 1110 | 1764 | 1/09/2004 | SL=IL | After Swatt/FK |
| GW0954 | OH94-1080I | 1655 | 906 | 1/09/2004 | SL=IL | After Swatt/FK |

### *4.4.8 Miscellaneous*

| Tape No | Dataset Name | Inline Range | Date Sent | SL/IL Rel | Remark. |
|---|---|---|---|---|---|
| CD #0008 | Depulse Filters | N/A | 15/07/04 | N/A | All three surveys |
| CD #0009 | Velocity Archive | All | 20/05/04 | SL=XL | FMIG_VELS_ANTARES TMIG_VELS_ANTARES |
| GS9981 | G1324PST40RMIG.3 | 1019-1969 | 01/09/04 | SL=IL | Minerva Area Rotated to Minerva Grid |
| GS9982 | G1324PST40FMIG.3 | 1019-1969 | 01/09/04 | SL=IL | Minerva Area Rotated to Minerva Grid |
| GS9983 | G1324PST40RNER.3 | 1019-1969 | 01/09/04 | SL=IL | Minerva Area Rotated to Minerva Grid |
| GS9984 | G1324PST40RFAR.3 | 1019-1969 | 01/09/04 | SL=IL | Minerva Area Rotated to Minerva Grid |
| GS9985 | G1324PST40RMID.3 | 1019-1969 | 01/09/04 | SL=IL | Minerva Area Rotated to Minerva Grid |
| GS9980 | G1324PST40RMID.4 | 954 - 1432 | 08/11/04 | SL=IL | Final Full Fold Migrations Sorted to Antares3D Inline Grid |
| CD #0011 | P6/98 & Final Report | | 08/11/04 | | P6/98 & Final Processing Report |